

主動矩陣有機發光二極體於薄膜電晶體之補償驅動電路研究

研究生：竹立煒

指導教授：劉柏村 博士

國立交通大學光電工程學系光電工程研究所

摘要

有機發光二極體(organic light-emitting diodes, OLEDs)顯示器是使用有機化合物堆疊，利用電子電洞對在發光層結合而能夠發出光線之平面顯示器，有機發光二極體顯示器具有體積小、重量輕、可視範圍廣、高對比、高反應速度、低操作電壓、可撓以及簡易製作等優點。主動矩陣式有機發光二極體顯示器是利用電晶體與 OLED 結合驅動的面板，OLED 需要由電流源來驅動電致發光，流經電晶體之電流量的變異對於主動矩陣式有機發光二極體顯示器的亮度均勻有負面的影響，因此，畫素驅動電路的品質對於主動矩陣式有機發光二極體顯示器之畫質非常重要。傳統的 AMOLED 顯示器的操作模式為兩個薄膜電晶體(thin film transistor, 簡稱 TFT)，分別作為開關與驅動元件，另外搭配一個儲存電容，然而無論使用有機薄膜電晶體(Organic TFTs, 簡稱 OTFT),非晶態薄膜電晶體 (hydrogenated amorphous TFTs, 簡稱 a-TFT:H)，或者是低溫複晶態薄膜電晶體 (low temperature poly TFTs, 簡稱 LTPS)，都有其無法克服的缺點；LTPS 電子遷移率高，使得元件尺寸可以縮小，提升開口率，降低操作電壓，達到省電目的，但其製程成本較高，而且均勻度不佳。另一方面，a-TFT:H 擁有較高的均勻度和較低的製程成本，然而 a-TFT:H 本身遷移率不高，以及所

需驅動開關之跨壓很大，而 OTFT 是很新穎的元件，不只成本較低且可在低溫下製作，所以其為可撓式基板驅動元件，但相對均勻性以及遷移率在此三者中是最差的，當面板在長時間操作下，各種驅動元件 (driving TFT) 會因為劣化造成臨界電壓(threshold voltage)的漂移以及遷移率的劣化，使得整個驅動電流越來越小，面板壽命變短，因此用以補償臨界電壓與對於不同電晶體形態設計適當驅動電路正被廣範研究中

在本篇論文，提出了三種驅動補償電路，分別使用 LTPS 和 OTFTs 為驅動元件，且設計是利用元件本身特性的優缺點與結合系統於玻璃上之技術(SOG)，以其有效改善面板畫面亮度不均勻，以及可靠度不佳再加上高成本的問題，此將成為大型顯示與可撓式面板的前瞻思想。



Research of AMOLED pixel compensation circuit using TFTs

Student : Li-Wei Chu

Advisor : Po-Tsun Liu

Department of Photonics&Institute of Electro-Optical Engineering
National Chiao Tung University

Abstract

The emission mechanism of organic light-emitting diode (OLED) is using stacked organic material while electron-hole pairs combine in the emission layer then it scatters the light. OLED displays have recently attracted much attention. Because OLED has thin module, light weight , high contrast ratio, wide viewing angle, fast response time, low operation voltage, flexible and simple fabrication. Active matrix organic light emitting diode (AMOLED) displays that integrate OLED and transistors are quite popular today. OLED needs stable current source which is given by transistors to drive, thereby, it will have negative effects for AMOLEDs uniformity of illumination if the driving current varies with the transistors degradation. So, the quality of pixel driving circuit is very important. The operation of conventional AMOLED display panels are two thin film transistors (TFTs) , which are individually for switching, driving function, and accompany with a storage capacitor. However, no matter organic TFTs (OTFTs) ,hydrogenated amorphous TFTs (a-TFTs:H) or low temperature poly TFTs (LTPS) we use, they have their own obstacles. The significant advantages over LTPS are high mobility, large

aperture ratio and lower operation voltage makes power conservation. But the drawbacks are higher cost on fabrication and lower uniformity. In other hand, a-TFTs:H have good uniformity and low cost, nevertheless, the lower mobility (about $1 \text{ cm}^2/\text{v.s}$) and large on/off switch operation voltage are the shortcomings. Finally, OTFTs are not only low cost but also could be fabricated in low temperature which really suit for novel flexible applications. But the uniformity and mobility are the worst over the three types before. All of the driving TFT would cause threshold voltage shift and electron properties degradation after long time operation. It leads the driving current becomes lower, so the pixel compensation circuits for such defects have been extensively studied nowadays.

In this thesis, we introduce three Voltage-Programmed Pixel Circuits (VPPCs). The transistors are employing LTPS and OTFTs respectively. The design rules are based on the device properties and combined with the concept of System On Glass (SOG). We except for improving panels' uniformity, reliability and reduce the cost. It will give advanced cerebration for the large size and flexible displays.

Acknowledgements

學生誠摯的感謝指導教授劉柏村及統寶光電劉炳麟學長，老師與學長用心的教導元件製程與 AMOLED 驅動電路設計的理念，而每個禮拜的 meeting 討論及指導，使我在這兩年中受益良多。老師學問不僅淵博且對待事務的嚴謹是我們努力學習的典範。感謝帶過我的學長們：盧皓彥和鄒一德學長對我的教導，且總能在我有疑問給予適當意見，無論是在元件機制，製程整合，或是電路模擬，這兩年讓我學到許多且相當充實。也感謝 DADS 實驗室鄭枷彬、何漢清、李允祥同學及本實驗室豫杰、阿貴(康康)、尚祐、繼聖、誼明、逸侑、超駿、威廷、巍芳、逸立的幫忙，因為有你們一起修課，一起打球，一起做實驗使我在學校的生活更充實，而學弟小豬豬、小劉、虛胖、阿寶和我共同研究三國歷史以及一起參加運動比賽，紓解了我的課業與實驗的壓力，無疑是研究生涯中最好的同伴。

女朋友姿妤的支持更是我前進的動力，雖然姿妤情緒有時會有些不穩定但是沒有姿妤的加油、陪伴，相信這兩年的生活無法過的如此順遂。最後，謹獻給我摯愛的雙親以及姊姊，無論發生了什麼事情，你們永遠陪在我身旁的，當我生病不舒服也會照顧我關心我，謝謝你們。

Contents

Chinese Abstract.....	I
English Abstract.....	III
Acknowledgements.....	V
Contents	VI
Figure Captions.....	VIII
<u>Chapter 1 Introduction</u>	
1.1 Background	1
1.2 Motivation	3
1,3 Thesis organization	4
<u>Chapter 2 Poly based compensation pixel circuit</u>	
2.1 Introduction	6
2.2 Combination of power & data line 4T1C circuit	
2.2.1 Pixel structure and timing scheme	7
2.2.2 Simulation results and discussions	9
2.2.3 Summary	11
2.3 Comprehensive 3T1C compensation circuit	
2.3.1 Pixel structure and timing scheme	12
2.3.2 Simulation results and discussions	14
2.3.3 Summary	15

Chapter 3 OTFT based compensation pixel circuit

3.1 Device of OTFT

3.1.1 Overview of OTFT 30

3.1.2 Process Flow Of Organic Thin Film Transistors
Fabrication 30

3.1.3 Organic Thin Film Transistors Parameter Extraction 31

3.1.4 Measurement and SPICE model of OTFT 32

3.2 Complementary Voltage Induce Coupling Driving

3.2.1 Pixel structure and timing scheme 34

3.2.2 Simulation results and discussions 36

3.2.3 Summary 38

Chapter 4 Conclusions and Future works 46

References 48

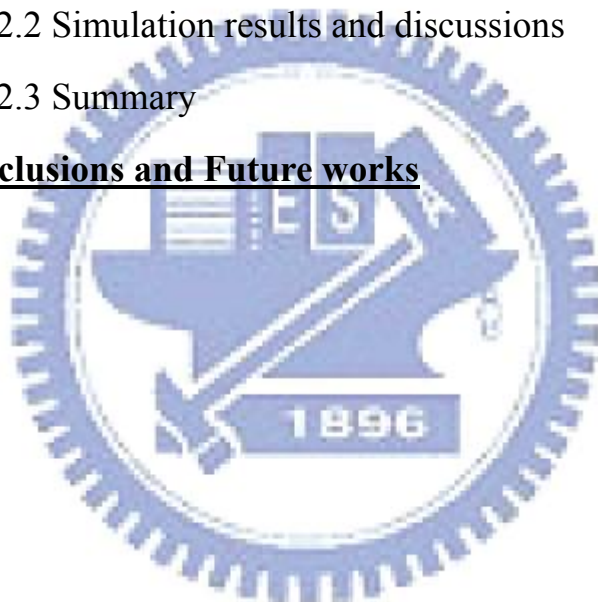


Figure Captions

Chapter2

Fig. 2-1 Schematic of the proposed pixel circuit and controlling signals.....	17
Fig. 2-2 External driving way for reducing one switch panel scheme diagram.....	18
Fig. 2-3 (a) was the I_D-V_G and (b) was I_D-V_D	19
Fig. 2-4 V_t shift plot of our driving transistor model with $V_D = -5V$ and the shift value was between $\pm 1V$	20
Fig. 2-5 The transient simulation result of driving transistor (T1) with threshold voltage (a)-2V and (b)-3V.	21
Fig. 2-6 The change of driving current versus operation time with variant threshold voltage. Driving current was 0.984uA, 0.998uA, and 1.014uA corresponding to $V_t = -1, -2$ and $-3V$, respectively.....	21
Fig. 2-7 (a) I_D-V_D plot of driving transistor T1. 1uA was set as the standard driving current. At the beginning, $V_{sd} = 8.2V$ for T1, then we fed $V_{DATA} = 2.4V$ for the next row (V_{sd} became 5.8V). The variation of current was just 4.4 nA as seen in Fig.2-7(b) clearly, so the proposed circuit could decrease the voltage variation from power data line voltage variation.	22
Fig. 2-8 represented output current of proposed pixel and conventional pixel at different threshold voltage shift.	22
Fig. 2-9 shows the driving method of proposed circuit.....	23
Fig. 2-10 Schematic of the proposed pixel circuit and controlling signals.	24
Fig. 2-11 shows the parallel driving scheme.....	24
Fig. 2-12 depicts panel arrangement of 3T1C structure with additional	

multiplexer and current mirror structure compared with traditional AMOLED	25
Fig. 2-13 The transient simulation result of driving transistor (MD).	26
Fig. 2-14 The change of driving current versus operation time with variant threshold voltage. Driving current was 0.98uA, 0.986uA, and 0.999uA corresponding to $V_t = -1$, -2 and $-3V$	26
Fig. 2-15 states current error versus threshold voltage among $-2\pm 1V$ with driving current (a) 0.25uA, (b) 0.5uA, (c) 0.75uA and (d) 1uA.	27
Fig 2-16 states current error versus mobility among $85\pm 4 \text{ cm}^2/V.s$ with driving current (a) 0.25uA, (b) 0.5uA, (c) 0.75uA and (d) 1uA..	28
Fig.2-17 presents the current error of MD among the data range $-0.6V\sim 0.6V$ for threshold voltage $-1V$ and $-3V$. Error rate is all less than 2.9% to reveal superior information of our study.	29

Chapter3

Fig. 3-1 shows the cross-sectional view of a top contact & bottom gate OTFT structure.....	40
Fig. 3-2 (a) and (b) are the I_D-V_G and I_D-V_D of the experiment results respectively.	40
Fig. 3-3 The TFT RPI model for HSPICE simulation (Level=62) shows I_D-V_G plot.	41

Fig. 3-4 shows the measured and simulated characteristics of the OTFT devices.....41

Fig. 3-5 depicts a schematic diagram of the proposed pixel circuitry.42

Fig. 3-6 V_t shift plot of our driving transistor model with $V_D = -10V$ and the shift value is between $\pm 1V$42

Fig. 3-7 (a) Measured and simulated output characteristics of pentacene-based OTFT for different gate voltage.(b) The change of driving current (IOLED) versus operation time for the OTFTs with variant threshold voltages in the proposed pixel circuit. IOLED is 1.016 μA , 0.998 μA and 0.9852 μA for $V_t = -0.5V$, $-1.5V$ and $-2.5V$, respectively. (c) The current ranging from 0.97 μA to 1.03 μA43

Fig. 3-8 Transient waveforms at specific nodes in the proposed pixel circuit while the input data was set to (a) $V_{data} = 5V$ for generating 262 nA of driving current, and (b) $V_{data} = 17V$ for generating 1 μA of driving current.44

Fig. 3-9 presents the current error of TD among the data range 1V~17V. It shows a good compensation function for the errors are all less than 2.9%.45

Fig. 3-10 represents output current of proposed pixel and conventional pixel at different threshold voltage shift.45

Chapter 1

Introduction

1.1 Background

The appearance of traditional monitors which called cathode ray tube (CRT) are hard to find nowadays. The multi-kind of flat-panel display technology are invented and developed to make our life more splendid. Among such advanced technology, thin film transistor liquid crystal display (TFT-LCD) [1]-[4] is the most well-established one. LCD displays have two areas of polarizing substance, and a liquid crystal solution in between. With the passing of electric current through the liquid, the crystals line up in such a way that light cannot infiltrate them. Each crystal acts like a shutter, either blocking the light or allowing it to come through. The cost of TFT-LCD is gradually decreasing by the vast investment of many enterprises and it makes the markets more competitive with the conventional displays. However, TFT-LCD still has some inevitable drawbacks, such as : narrow viewing angle 、 slow response time 、 low contrast and so on. As a result, Active matrix organic liquid crystal displays (AMOLED) [5] has attracted much more attention which consist of OLED pixels that have been deposited or integrated onto a thin film transistor (TFT) array to form a matrix of pixels that illuminate light upon electrical activation. In contrast to PMOLED display, where electricity is distributed row by row, the active-matrix TFT backplane acts as an array of switches that control the amount of current

flowing through each OLED pixel. The TFT array controls the current to flow the pixels, and signals to each pixel how brightly to shine. The benefits of AMOLED are lower power requirements, a less-expensive manufacturing process, improvements in contrast and color, and the ability to bend[6]. AMOLED doesn't need backlight, unlike TFT-LCD. OLED could illuminate by itself, so it can save power and without color filters.

Regardless of TFT-LCD or AMOLED, the devices (TFTs) are the major factor for driving and switching operation. The electronic properties of TFTs influence the performance of such displays. In General, hydrogenated amorphous TFTs (a-TFTs:H) [7]-[11] and low temperature poly TFTs (LTPS) [12]-[17]are ordinary consuming products. But next-generation technologies such as organic TFTs (OTFTs)[18]-[20] are also under development. A-TFTs:H have good uniformity and low cost, nevertheless, the lower mobility (about $1 \text{ cm}^2/\text{v.s}$) and large on/off switch operation voltge are the shortcomings. However the significant advantages over LTPS are high mobility, large aperture ratio and lower operation voltage makes power conservation. But the drawbacks are higher cost on fabrication and lower uniformity. Eventually, OTFTs are not only low cost but also could be fabricated in low temperature which really suit for novel flexible applications. But the uniformity and mobility are the worst over the three types before.

1.2 Motivation

The first active pixel circuit was using one transistor and one storage capacitor (1T1C) to drive. The operation mechanism was when the scan line turned on the driving data will charge the capacitor until it turned off. After this, driving current was just releasing charge by the RC constant, so it could not hold constant driving current (the illumination of this was defined by mean integrated value) in one frame time. Consequently, the 2T1C pixel circuit based on one driving, one switch and one storage capacitor was proposed to improve the drawback before. For OLED structure, the indium-doped tin oxide (ITO) transparent anode of the OLED deposit firstly on the active-matrix substrate because the sputtering of ITO would degrade the organic layer. In most hydrogenated amorphous TFT-OLED, the anode of OLED is connected to the source node of TFT. Hence, 2T1C pixel circuit based on n-type TFTs must consider not only the OLED but also driving transistor threshold voltage shift problem because the driving current is controlled by V_{GS} (V_S was getting higher when OLED threshold voltage raised for long time driving), So, 2T1C employed p-type TFTs (Poly and OTFT phase, there was no p-type amorphous TFTs) could eliminate the .OLED threshold voltage raising problem but it still had the other one.

Although the promising evolution of display technology, AMOLED still has various demerits which scientists have to solve these. If TFTs are set as the AMOLEDs driving element, the threshold voltage shift and device degradation are unwanted for the pixel circuits. For the reason, compensation pixel circuits have been proposed to modify 2T1C circuits.

And numerous compensation methods have been developed such as voltage modulation [21]-[26] ,current programming methods. [27] [28] and clamp inverter methods[29][30].The current driving methods compensates all the electronic properties , but the longer settling time at low data current increases the frame time so it is not suitable for practical use in high resolution displays. Secondly, the clamp inverter driving way could reduce the transistor effect lowest (Because it operates in linear region), but it consumes more power, gray scale is uneasy to adjust and sacrifices light emitting time so it carries out rarely. Therefore, without the settling time problem and lower power consumption make voltage driving becoming commonly implemented nowadays, but it still exists imperfect compensation [31] during the V_t generation cycle. In this thesis, we propose three novel Voltage-Programmed Pixel Circuits (VPPCs) to enhance the degradation of OLED output current. The transistors of them are employing LTPS and OTFTs respectively.

1.3 Thesis organization

Chapter 1 Introduction

1.1 Background	1
1.2 Motivation	3
1,3 Thesis organization	4

Chapter 2 Poly based compensation pixel circuit

2.1 Introduction	6
2.2 Combination of power & data line 4T1C circuit	
2.2.1 Pixel structure and timing scheme	7

2.2.2 Simulation results and discussions	9
2.2.3 Summary	11
2.3 Comprehensive 3T1C compensation circuit	
2.3.1 Pixel structure and timing scheme	12
2.3.2 Simulation results and discussions	14
2.3.3 Summary	15
Chapter 3 OTFT based compensation pixel circuit	
3.1 Device of OTFT	
3.1.1 Overview of OTFT	30
3.1.2 Process Flow Of Organic Thin Film Transistors Fabrication	30
3.1.3 Organic Thin Film Transistors Parameter Extraction	31
3.1.4 Measurement and SPICE model of OTFT	32
3.2 Complementary Voltage Induce Coupling Driving	
3.2.1 Pixel structure and timing scheme	34
3.2.2 Simulation results and discussions	36
3.2.3 Summary	38
Chapter 4 Conclusions and Future works	46
References	48

Chapter 2

Poly based compensation pixel circuit

2.1 Introduction

Poly-Silicon backplane technology is a technology-of-choice for OLEDs today because it provides excellent mobilities that meet OLED current drive requirements. Poly-Si technology also allows for the integration of the drive circuitry directly onto the substrate. There are several key challenges, however, to address: reducing threshold voltage non-uniformities of poly-Si, installing additional manufacturing capacity, and demonstrating commercially-viable manufacturing yields. With these issues resolved, poly-Si AMOLEDs should offer excellent performance as some early-stage prototypes and products suggest.

Poly-silicon TFTs have been widely considered for AMOLED due to their high current capability [32],[33] and could fabricate driving circuit at panel periphery to achieve system on panel (SOP). However, the excimer laser annealing (ELA) facility causes nonuniformity of active layer lead different threshold voltage to each transistor. In addition, large-size panel drives higher current to let power voltage (VDD) depends on the position and degrades driving current. These instabilities emphasize the importance of compensation circuit. In previous work, compensation circuits present current driving, clamp inverter driving and voltage driving ways[21]-[30]. Firstly, the current driving way compensates electronic properties better, but the longer settling time [34] at low data current increases the frame time so it is not suitable for

practical use in high resolution displays. Secondly, the clamp inverter driving way could reduce the transistor effect lowest (Because it operates in linear region), but it consumes more power, gray scale is uneasy to adjust and sacrifices light emitting time so it carries out rarely. Therefore, without the settling time problem and lower power consumption make voltage driving becoming commonly implemented nowadays, but it still exists imperfect compensation [31] during the V_t generation cycle. In our study, we propose two types of compensation circuit. Firstly, we merge power line and data line which based on holding source and drain voltage of the driving transistor during data variation in a frame time and compensate threshold voltage shift in voltage driving way. Furthermore, a notion of external driving is demonstrated to decrease transistors in pixel region while employing ink-jet printing technique to pattern OLED cathode. Secondly, voltage and current hybrid driving pixel circuit is proposed to overcome threshold voltage shift and mobility degradation use only 3T1C structure. Because of such comprehensive advantage, the sacrifice is emission time of OLED so the parallel driving scheme in order to decrease the non-ideal effect is proposed.

2.2 Combination of power & data line 4T1C circuit

2.2.1 Pixel structure and operation

Fig. 2-1 depicts a schematic diagram of the proposed pixel circuitry. The inner of the dash square indicates a pixel region with a driving transistor T1, and three switch T2, T3, and T4. The switch T5 was designed to be outside the pixel area. The operation principle could be divided into three periods, including releasing charge, threshold voltage

(V_t) generation/ current regulation, and driving. In the first period, SCAN1 and SCAN2 were set to low and high to turn on the T2 T3 and T4 turns off respectively. T5 was controlled in the on state by the EM signal. The switch T3 connected to SCAN1[n-1] in order to buffer the voltage so as to design the turn on voltage same with power data line highest voltage (10V). In this released charge period, voltage of node A went to lower value. The arrangement of switch T5 showed in Fig.2-2 was fabricated by the cathode pattern process, located at the right side of an external pixel area. Therefore, the actual device layout in a pixel region only consisted of four transistors. Such an arrangement of external driving circuit could decrease the manufacture complexity for each display pixel.

In the V_t generation/current regulation period, SCAN1 was still kept low, and T2 and T3 were kept in the turn-on state. SCAN2 still high let T4 off, and T5 turned off, respectively. The power data line was given $V_{DD}-V_{DATA}$. With the diode-connection the voltage of node A went to $V_{DD}-V_{DATA}-|V_{tp}|$. In the driving period, SCAN1 is set to high to turn off T2 and T3. At the same time, SCAN2 was set to low to turn T4 on. T5 was at the on-state. Voltage of power data line returned to V_{DD} , and then the voltage of storage capacitor was shown as followed.

$$V_{SG} = V_{DD} - (V_{DD} - V_{DATA} - |V_{tp}|) = V_{DATA} + |V_{tp}|$$

$$I_{OLED} = K(V_{SG} - |V_{tp}|)^2 = K(V_{DATA} + |V_{tp}| - |V_{tp}|)^2 = K(V_{DATA})^2 \quad (2-1)$$

Where $|V_{tp}|$ was the threshold voltage of poly TFT and $K=0.5\mu p Cox$

The above formula clearly indicated that the proposed compensation circuit could have higher immunity to the threshold voltage variation and due to fixing among the source and drain voltage of driving transistor (T1)

that gave stable driving current for each pixel row even power data line with large variation for next row. Nevertheless, we should assume T1 operated in saturation region all the time, so, we designed V_{EE} sufficient lower (Ex $V_{EE} = -5V$).

2.2.2 Simulation Results

The HSPICE software with the RPI poly-silicon TFT model (Level=62) were used to verify the proposed circuit. The mobility and threshold voltage of DTFT were $80 \text{ cm}^2/V\cdot\text{s}$ and $-2V$. Cst was set to 350 fF , Vdd and the high level of the signals ([n]Scan and [n]EM) were set as $10V$, respectively. The aspect ratio of switch T2 was $5/5+5 \text{ um}$ using dual gate structure to decrease leakage current and other switches were all $5/5 \text{ um}$. The driving transistor was designed as $4/40 \text{ um}$ to reduce the non-ideal Kink effect for longer channel length. Fig.2-3(a) was the I_D-V_G and (b) was I_D-V_D of our simulation model, and Fig.2-4 gave a information for Vt shift plot of our driving transistor model with $V_D = -5V$ and the shift value was between $\pm 1V$. The transient simulation result of driving transistor(T1) with threshold voltage $-2V$ and $-3V$ was shown in Fig.2-5(a) and (b). The gate voltage of T1 was $2V$ in the first released charge period, then it generated threshold voltage through the diode-connection in the second period. A coupling effect occurred when it changed to the driving period. The plot exactly proved our design rule we mentioned in 2.2. Fig.2-6 presented the transition of driving current ($V_{DATA}=2.4V$ with $I=1\mu A$) versus operation time for variant threshold voltages ($\pm 1V$) in the proposed pixel circuit architecture. The first phase ($0\sim 5\mu s$) was releasing charge. Three different levels of current were presented, because the poly-TFT has distinct threshold voltage values.

With the diode-connection method to generate V_t and data feeding, the current gradually goes to zero in the second phase. At the third stage of driving period, driving current was 0.984 μ A, 0.998 μ A, and 1.014 μ A corresponding to $V_t = -1, -2, \text{ and } -3\text{V}$ respectively. The variation of driving current (ΔI) could be calculated less than 1.6%. This result showed the proposed pixel circuit was independent of threshold voltage values. Besides, we used longer channel length for the driving transistor to avoid non-programming row with disturbance which was caused by Kink effect. Fig.2-7(a) showed the I_D - V_D plot of driving transistor T1. 1 μ A was set as the standard driving current. At the beginning, $V_{sd} = 8.2\text{V}$ for T1, then we fed $V_{DATA} = 2.4\text{V}$ for the next row (V_{sd} became 5.8V). The variation of current was just 4.4 nA as seen in Fig.2-7(b) clearly, so the proposed circuit could decrease the voltage variation from power data line voltage variation. Fig.2-8 represented output current of proposed pixel and conventional pixel at different threshold voltage shift. This simulation result showed that OLED current in proposed pixel degrades from 1 μ A to 0.972 μ A while OLED current in 2T1C conventional pixel degraded lower than 0.03 μ A, so the circuit really had excellent compensation ability to reduce the current nonuniformity. Finally, we talked about the instability part. Because voltage of node A was a key point of controlling the driving current so we analyzed it. The switch-induced error voltage was mainly produced by charge injection and clock feedthrough[34][35]. Because we used small-size switches, the charge injection could be neglected for simply. In the end of V_t generation/current regulation period, T3 will be set to off and T4 to on state. The voltage source gave stable voltage so there was no feedthrough from T3 and T4. However the variation of

power data line and switch T2 made feedthrough respectively. Firstly, we assume T3 was on then T2 went off immediately. The initial voltage of node A was $V_{DD}-V_{DATA}-|V_{tp}|$, then

$$V_{A1} = V_{DD} - V_{DATA} - |V_{tp}| + \frac{C_{OV2}}{C_{GS1} + C_{GS2} + C_{OV1} + C_1} \Delta V \quad (2-2)$$

Where ΔV defined as interval of ON-OFF voltage, C_{OV1} and C_{OV2} were the overlap capacitances of T1 and T2[11]. Afterwards power data line changed to V_{DD} .

$$V_A = V_{A1} + \frac{C_{GS1}}{C_{GS1} + C_{OV2} + C_{OV1} + C_1} V_{DATA} \quad (2-3)$$

From the above formula, larger storage capacitor and smaller V_{DATA} variation reduced this non-ideality, besides the longer width of T2 resulted bigger C_{OV2} . So it was necessary to design appropriate channel width.

2.2.3 Summary

We propose a new 4T1C active-matrix organic light-emitting diode displays (AMOLEDs) pixel circuit using LTPS thin-film transistors is verified by SPICE simulation successfully. The pixel design compensates the variation of threshold voltage between $\pm 1V$ with 1.6% current non-uniformity. Besides, a proposed new external driving method and we combine power & data line for driving can reduce the number of switch transistors in a pixel and circuit complexity. Our proposed circuit reduces non-uniformity for driving OLED effectively, and the novel power data line diminishes not only layout area but also ESD conducting path to lower down the risk of destroying the pixel. Moreover, the proposed idea with the external driving can decrease transistors in pixel region and reduce the circuit complexity, while employing ink-jet printing technique to pattern OLED cathode.

2.3 Comprehensive 3T1C compensation circuit

2.3.1 Pixel structure and operation

First of all, we mention about the scan driver control in our study which defines the emission time of the panel. Scan signal is similar for TFT-LCD and AMOLED with each row time charging then driving with other times in each frame. Fig. 2-9 shows the driving method of our proposed circuit that program all row subsequent with emission period. Consequently, the effective emission time for OLED is lesser than traditional scheme. In this circumstance, the flicker won't be happened because of 60HZ for each frame is higher to avoid human eyes feeling fluctuation but the driving current should be designed higher to achieve the same luminance with conventional driving structure. Fig. 2-10 depicts a schematic diagram of the proposed pixel circuitry. M1 and M2 are switch transistors, MD is driving transistor. The operation principle is divided into three periods, including reference current (I_{ref}) generation, data feeding and driving. In the first period, SCAN1 were set to low to turn on the M1 and M2. In this reference current (I_{ref}) generation, data line is given V_{data} and voltage of node C goes to $V_{DD} - (I_{ref} / k_p)^{1/2} - |V_{tp}|$ because I_{ref} flows MD to derive equation of saturation region without the kink effect getting the value V_C . Where k_p is $0.5 \mu p C_{ox} W/L$, $|V_{tp}|$ is the absolutely threshold voltage of p-type poly TFT. In the data feeding period, SCAN1 turns off. Data line transfers to V_{ref} so V_C suffered a coupling effect to change MD's gate voltage with result to define magnitude driving current of OLED. In the third driving period, the V_{SG} of MD is

shown as followed.

$$\begin{aligned} V_{SG} &= VDD - (VDD - (I_{ref} / k_p)^{1/2} - |V_{tp}| + V_{ref} - V_{data}) \\ &= (I_{ref} / k_p)^{1/2} + |V_{tp}| + V_{ref} - V_{data} \end{aligned} \quad (2-4)$$

$$\begin{aligned} I_{OLED} &= k_p (V_{SG} - |V_{tp}|)^2 \\ &= k_p (I_{ref} / k_p)^{1/2} + |V_{tp}| + V_{ref} - V_{data} - |V_{tp}|)^2 \\ &= k_p [(I_{ref} / k_p)^{1/2} + (V_{ref} - V_{data})]^2 \\ &= I_{ref} + 2(k_p I_{ref})^{1/2} (V_{ref} - V_{data}) + k_p (V_{ref} - V_{data})^2 \end{aligned} \quad (2-5)$$

The above formula clearly indicated that the proposed compensation circuit could have higher immunity to the threshold voltage variation and mobility degradation using hybrid driving scheme. The item of k_p contains mobility information therefore the ability of compensated mobility degradation is especially completing at $V_{ref} - V_{data} = 0$ which means OLED driving current is just reference current (I_{ref}).

In the cause of the driving method (Fig 2-9) bring longer programming time, so we present parallel driving scheme to decrease this non-ideal effect. In former case of pixel compensation circuits are usually with two to four periods to operate the circuit function thereby we introduce the parallel driving scheme shown in Fig. 2-11 just with one period (about 5us) in each row time that really reduce the programming work to fit this circuit. The strong point of this voltage and current hybrid driving is about the settling time issue for pure current driving when low data current goes along with longer time to generate, so 5us will be same for total pixel in reference current (I_{ref}) generation duration it doesn't have settling time issue. Furthermore, hybrid driving must use more complicated IC or high pings increasing the cost. Look back to the reference current which is a constant value so it renders us to deposit current mirror structure outside the pixel region (Figure 2-12) simultaneous with pixel formation. This way is just need one ping to give

constant current and combine concept of system on glass (SOG).

2.3.2 Simulation Results

The HSPICE software with the RPI poly-silicon TFT model (Level=62) is used to verify the proposed circuit. The mobility and threshold voltage are $80 \text{ cm}^2/\text{V}\cdot\text{s}$ and -2V . Cst is set to 350 fF , Vdd is 10V and scan signal gives between $-5 \sim 10\text{V}$, respectively. The aspect ratio of switch is $5/5+5 \text{ um}$ using dual gate structure to decrease leakage current and the driving transistor is designed as $5/40 \text{ um}$ to reduce the non-ideal Kink effect for longer channel length. Fig 2-13 shows the transient waveform of MD consisted of three regions. In the region I, V_B and V_C are equal potential by turning on M1. The voltage is 1.127V corresponding to generate reference current ($I_{\text{ref}}=0.57\mu\text{A}$). V_B and V_C separate in next duration due to turning off M1 and M2. At this moment, data line changes to $V_{\text{ref}}=-0.67\text{V}$ so V_B is also coupled from 1.33V to 0.75V . V_C goes high result from MD without current through it. The third period is driving period, multiplexer transfer status let current go through OLED hence V_C goes low to maintain MD at saturation region. Fig 2-14 presents the transition of driving current ($I=1\mu\text{A}$) versus operation time for variant threshold voltages ($\pm 1\text{V}$) in the proposed pixel circuit architecture. The first phase ($10\sim 20\mu\text{s}$) is reference current generation. Three different levels of current are accumulated to I_{ref} , because the poly-TFT has distinct threshold voltage values. With M1 and M2 are turned off, I_{MD} goes to zero in the second phase. At the third stage of driving period, driving current was $0.98\mu\text{A}$, $0.986\mu\text{A}$, and $0.999\mu\text{A}$ corresponding to $V_t = -1, -2, \text{ and } -3\text{V}$ respectively. The variation of driving current (ΔI) could be

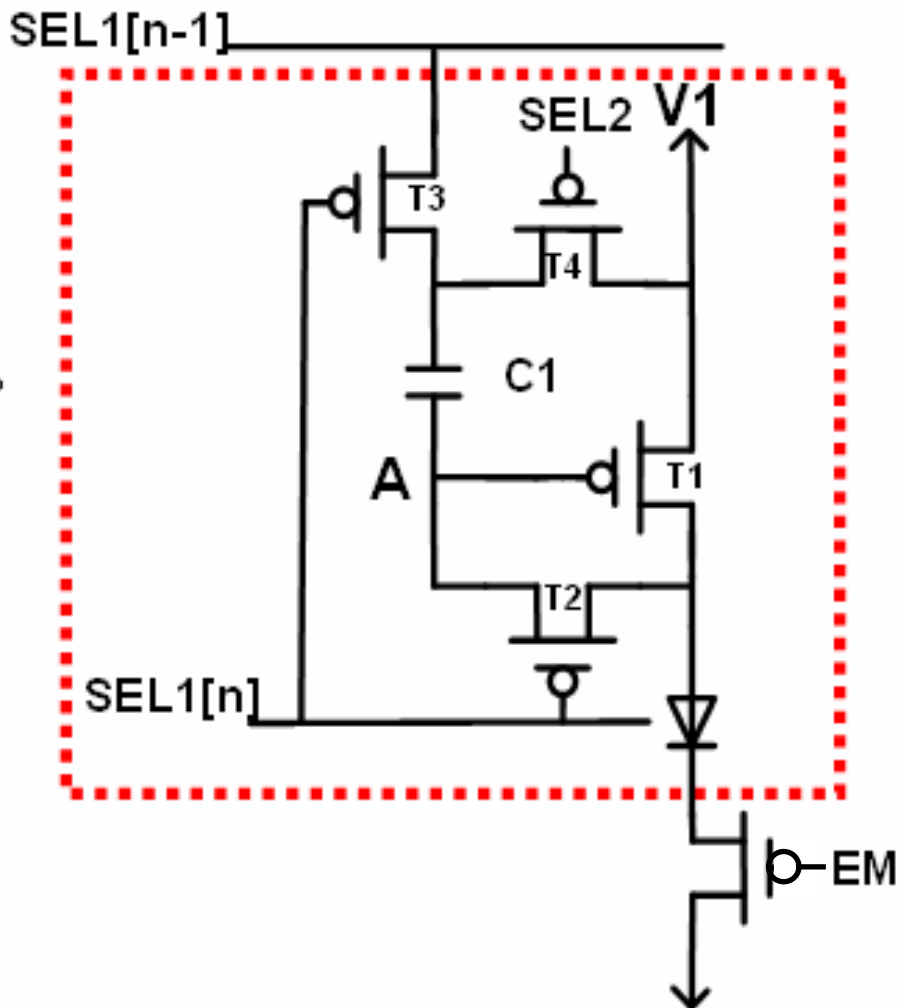
calculated less than 1.4%. This result showed the proposed pixel circuit was independent of threshold voltage values. Fig 2-15 states current error versus threshold voltage among $-2\pm 1V$ with driving current 0.25uA, 0.5uA, 0.75uA and 1uA. Solid line depicts voltage driving compensation in 2.2 and dash line is the proposed circuit. It could find dash line with higher compensation ability than solid line at V_t greater than $-2V$, but it is not obvious on the contrary. This asymmetric dash line is mainly caused by charging time. For 4T1C (VPPC), when absolute V_t is getting lower, $V_{DD}-V_{data}-|V_{tp}|$ is getting higher so the charging path becomes longer in v_t generation region. It would not affect proposed hybrid driving which is based on current driving scheme with reference current defines self threshold voltage and mobility generation. Totally, 3T1C supports better current error rate than conventional VPPC. Fig 2-16 states current error versus mobility among $85\pm 4\text{ cm}^2/V.s$ with driving current 0.25uA, 0.5uA, 0.75uA and 1uA. Solid line depicts circuit without mobility compensation function and dash line is the proposed circuit. It shows a nearly perfect statistics at $I = 0.5\mu A$ ($V_{data}=V_{ref}$) as mentioned before with error rate is just about 0.3%. Comprehensively, these four figures present row current error and verify our proposed circuit. Finally, Fig.2-17 presents the current error of MD among the data range $-0.6V\sim 0.6V$ for threshold voltage $-1V$ and $-3V$. Error rate is all less than 2.9% to reveal superior information of our study.

2.3.3 Summary

We propose a hybrid driving 3T1C active-matrix organic light-emitting diode displays (AMOLEDs) pixel circuit using LTPS thin-film transistors is verified by SPICE simulation successfully. The

pixel design compensates the variation of threshold voltage between $\pm 1V$ with 2.9% current non-uniformity among data range $-0.6V \sim 0.6V$. Besides, mobility degradation induced current non-uniformity is also decreased in our study especially at driving current is equal to reference current. Moreover, the proposed idea with parallel driving method release the programming time in a frame.





Clock table:

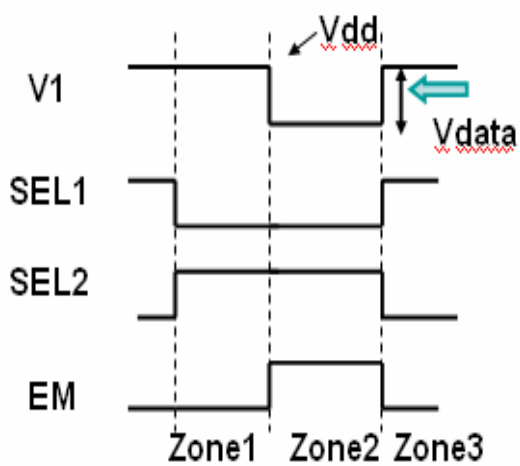


Fig. 2-1 Schematic of the proposed pixel circuit and controlling signals.

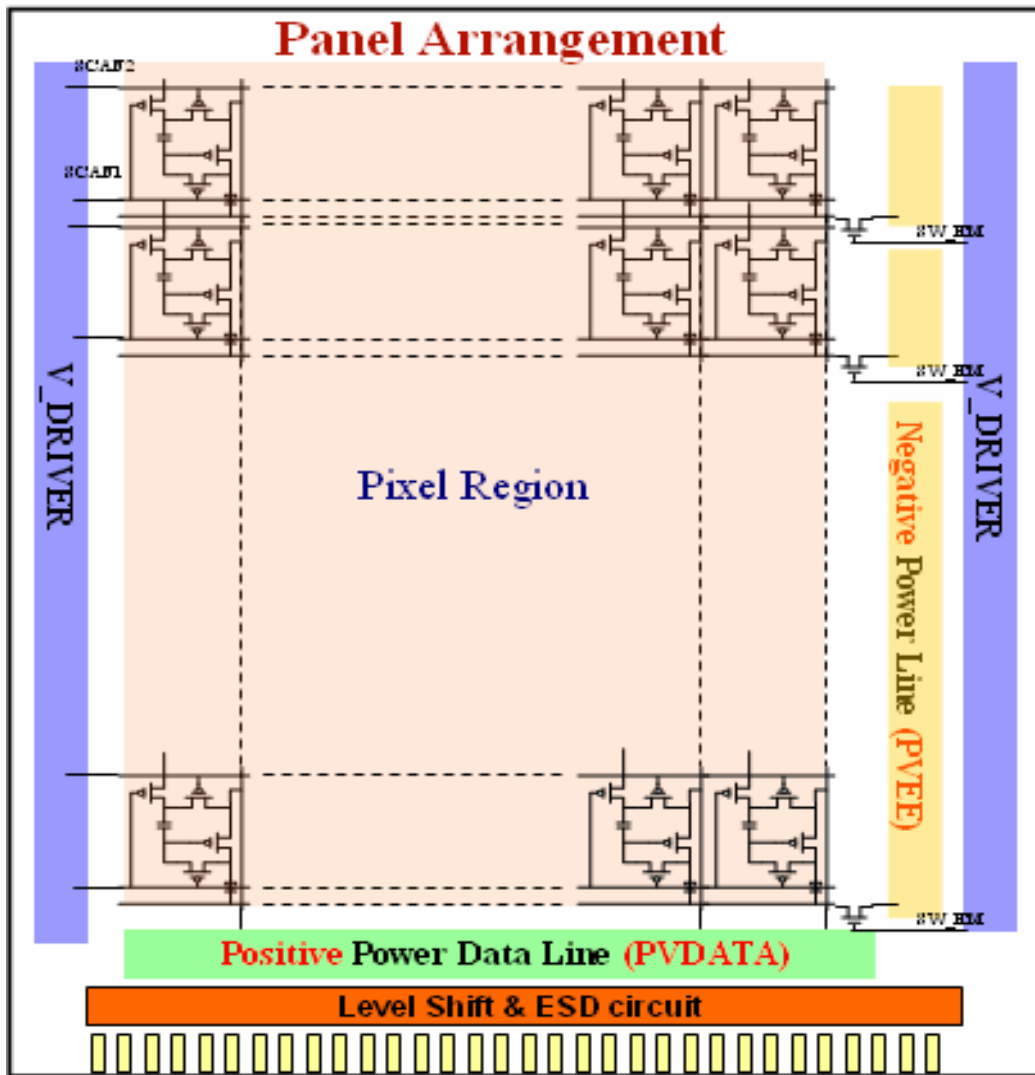


Fig. 2-2 External driving way for reducing one switch panel scheme diagram

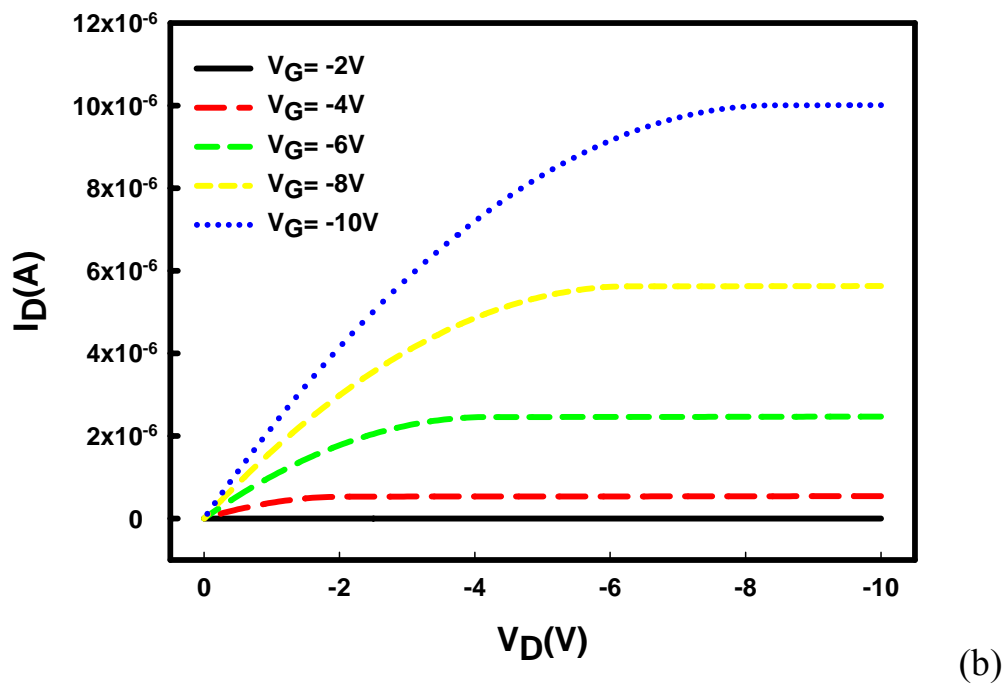
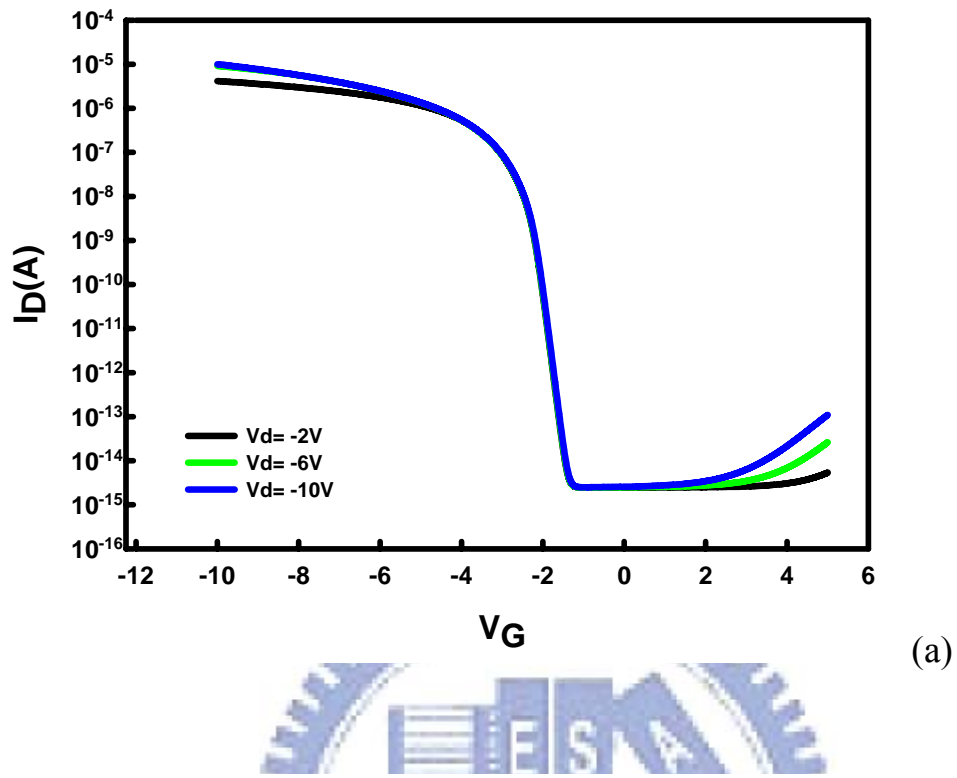


Fig.2-3(a) was the I_D - V_G and (b) was I_D - V_D

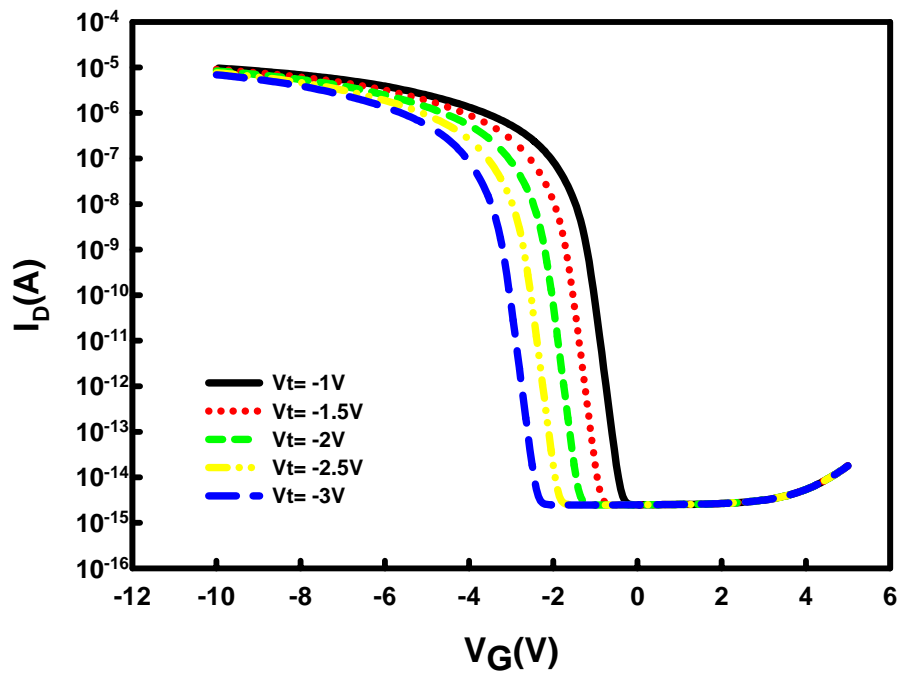
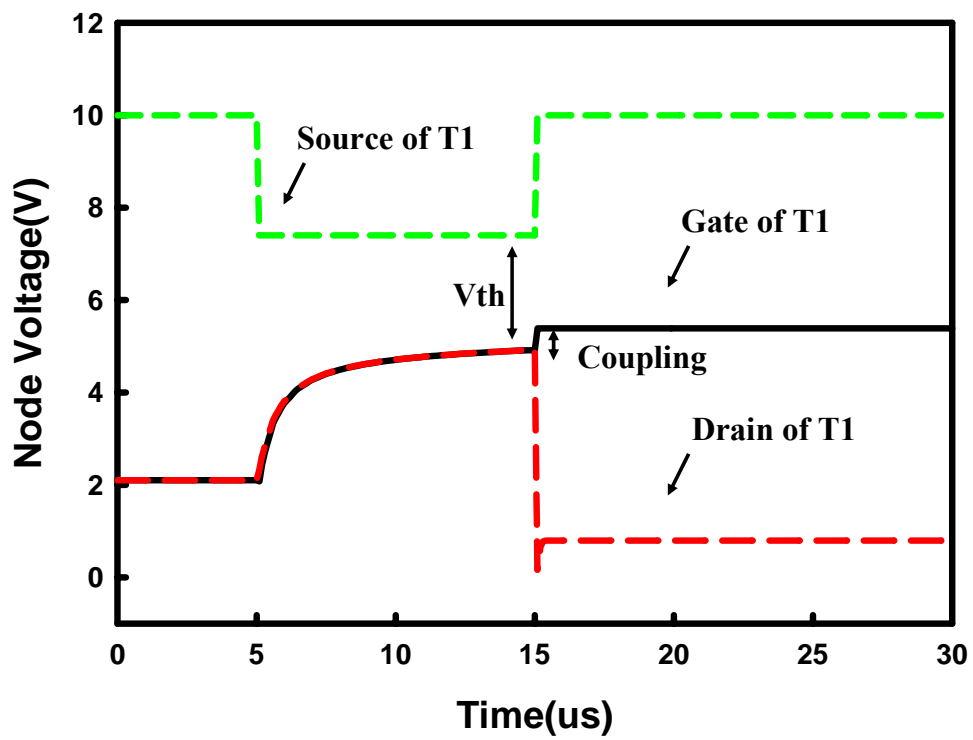
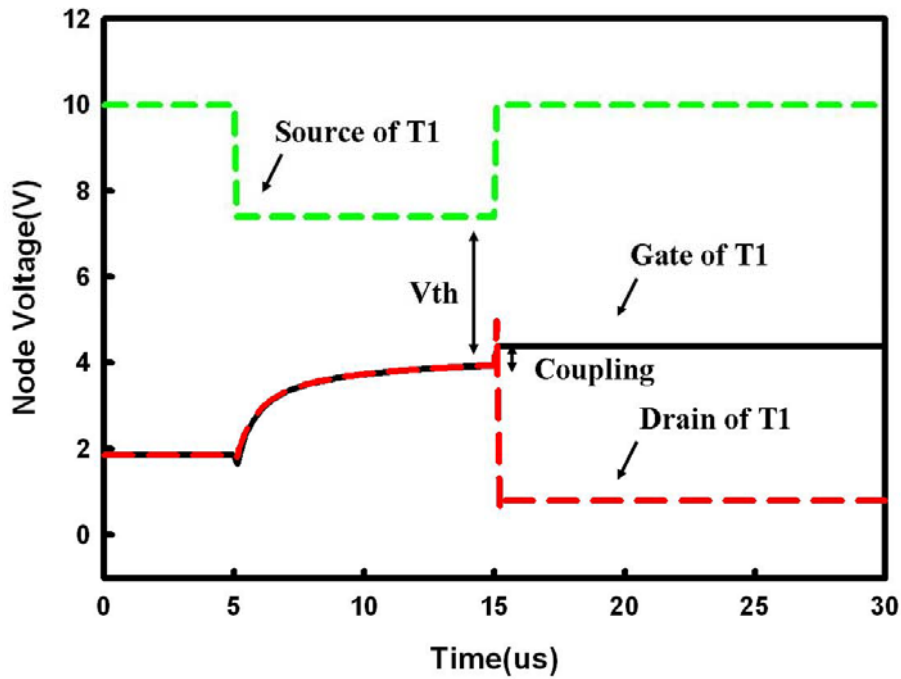


Fig.2-4 V_t shift plot of our driving transistor model with $V_D = -5V$ and the shift value was between $\pm 1V$



(a)



(b)

Fig.2-5 The transient simulation result of driving transistor(T1) with threshold voltage (a)-2V and (b)-3V.

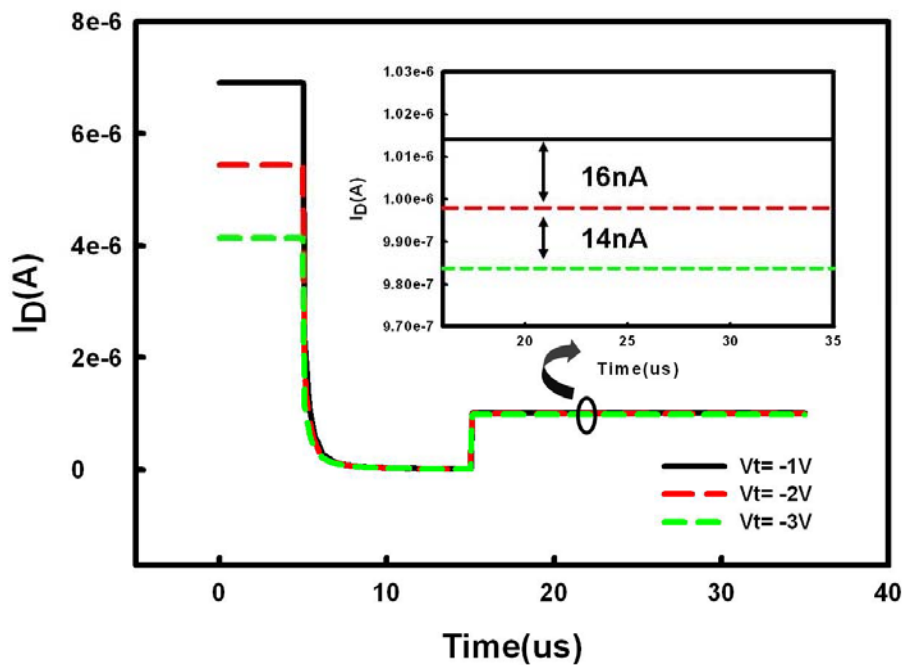


Fig.2-6 The change of driving current versus operation time with variant threshold voltage. Driving current was 0.984uA, 0.998uA, and 1.014uA corresponding to $V_t = -1$, -2 and $-3V$, respectively.

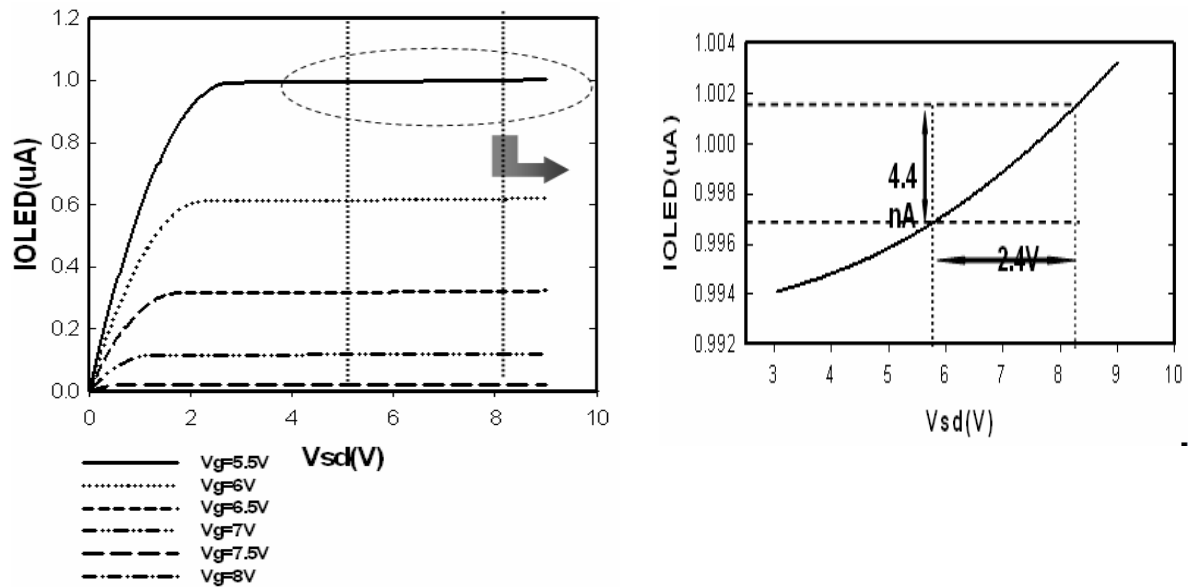


Fig.2-7(a) I_D - V_D plot of driving transistor T1. 1μA was set as the standard driving current. At the beginning, $V_{sd} = 8.2V$ for T1, then we fed $V_{DATA}=2.4V$ for the next row (V_{sd} became 5.8V). The variation of current was just 4.4 nA as seen in Fig.2-7(b) clearly, so the proposed circuit could decrease the voltage variation from power data line voltage variation.

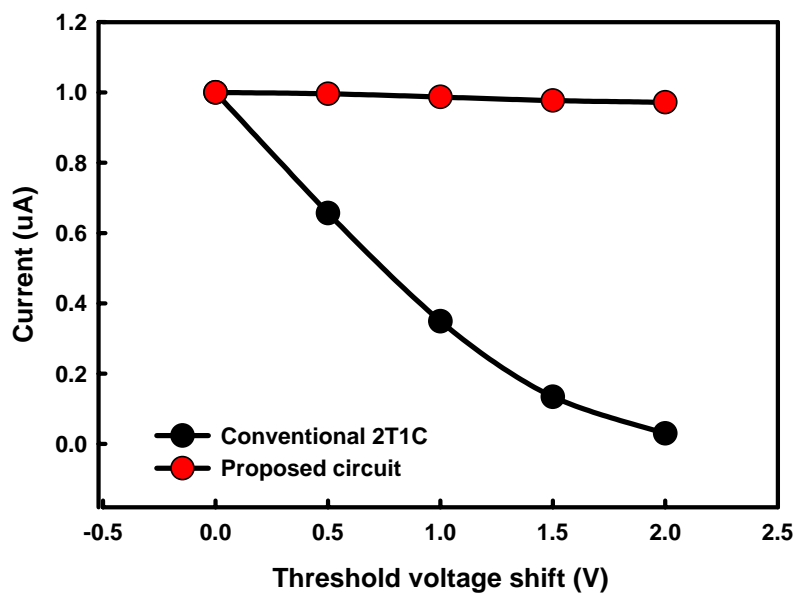


Fig.2-8 represented output current of proposed pixel and conventional pixel at different threshold voltage shift.

Driving method

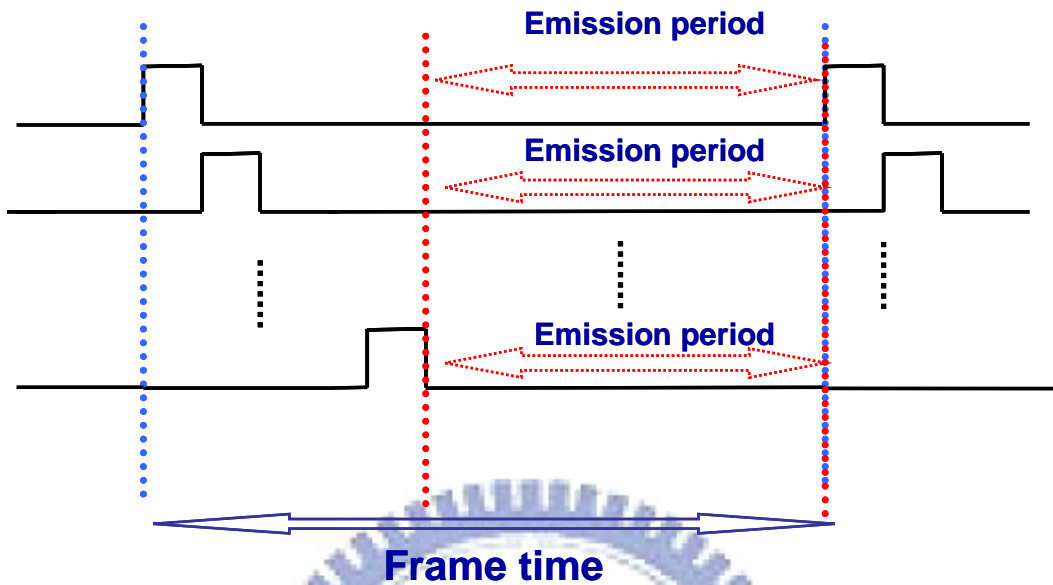
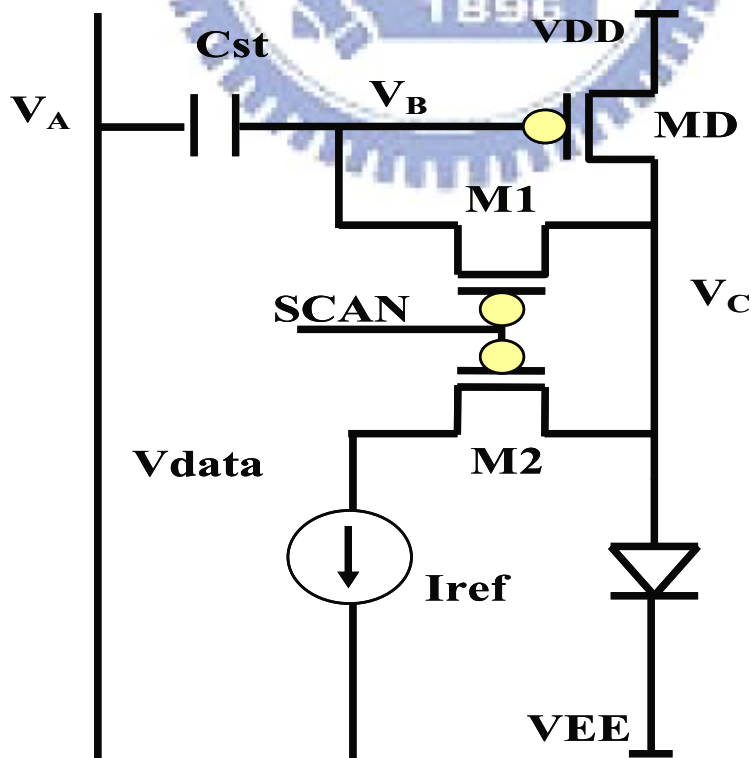


Fig. 2-9 shows the driving method of proposed circuit

3T1C (Poly-TFT)



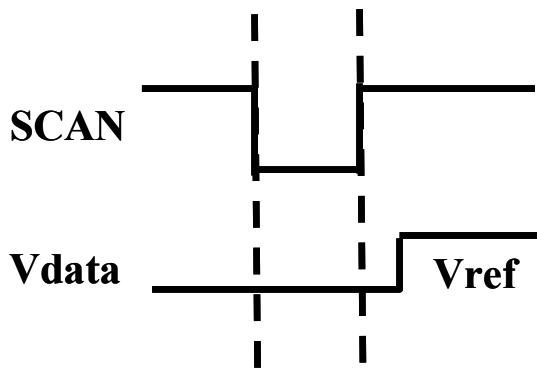


Fig. 2-10 Schematic of the proposed pixel circuit and controlling signals.

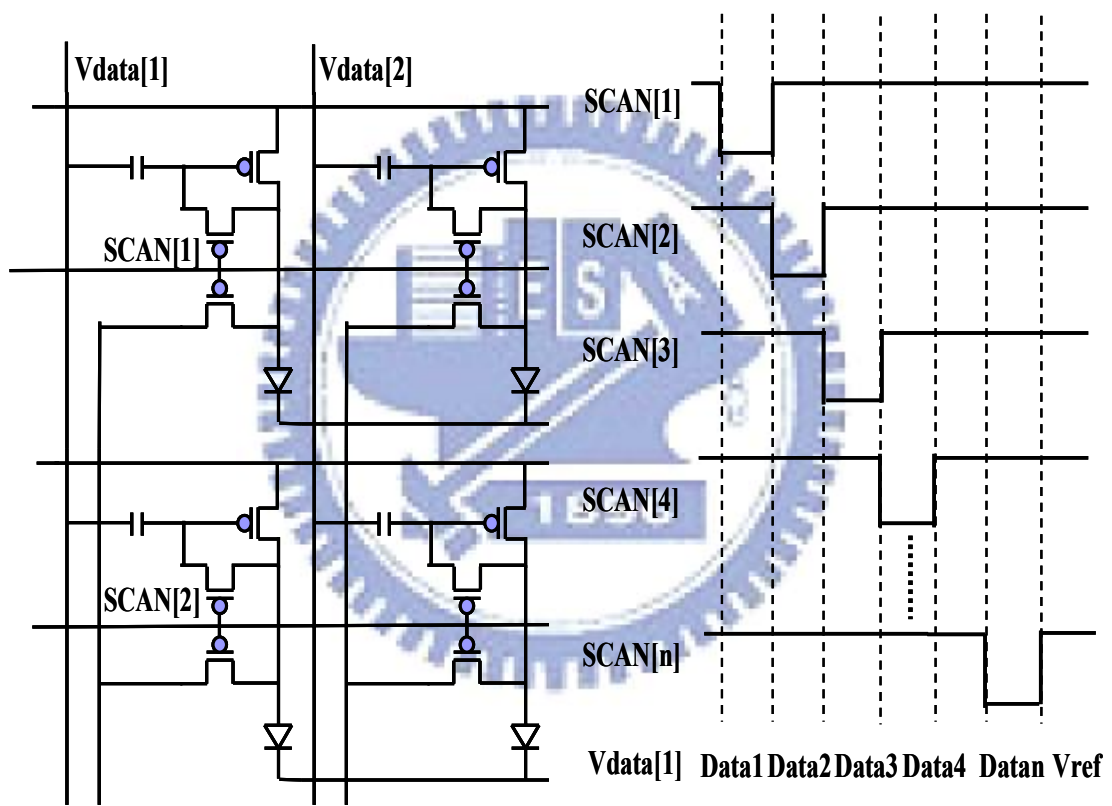


Fig. 2-11 shows the parallel driving scheme

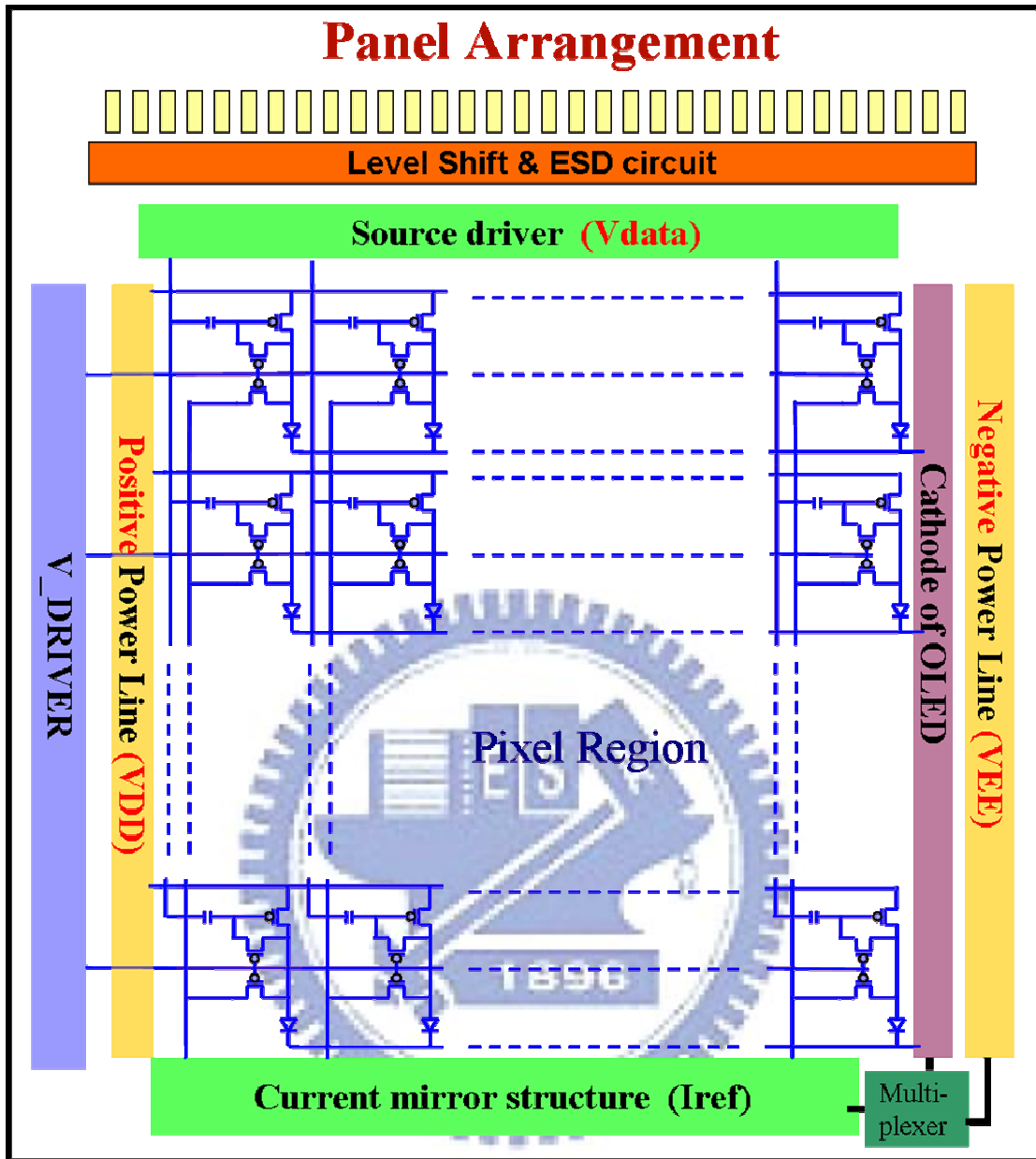


Fig 2-12 depicts panel arrangement of 3T1C structure with additional multiplexer and current mirror structure compared with traditional AMOLED

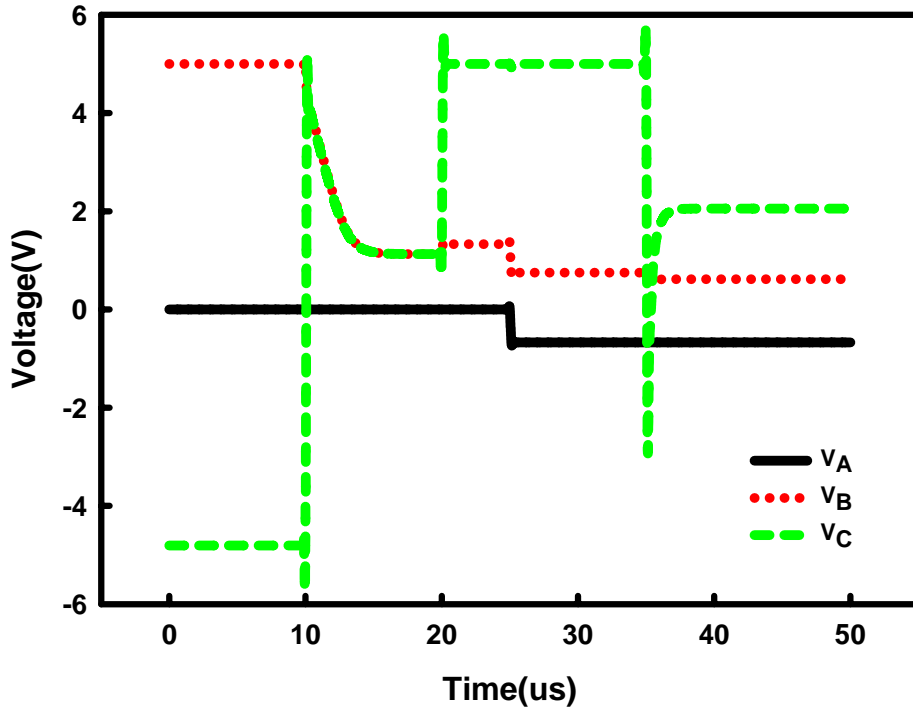


Fig.2-13 The transient simulation result of driving transistor (MD)

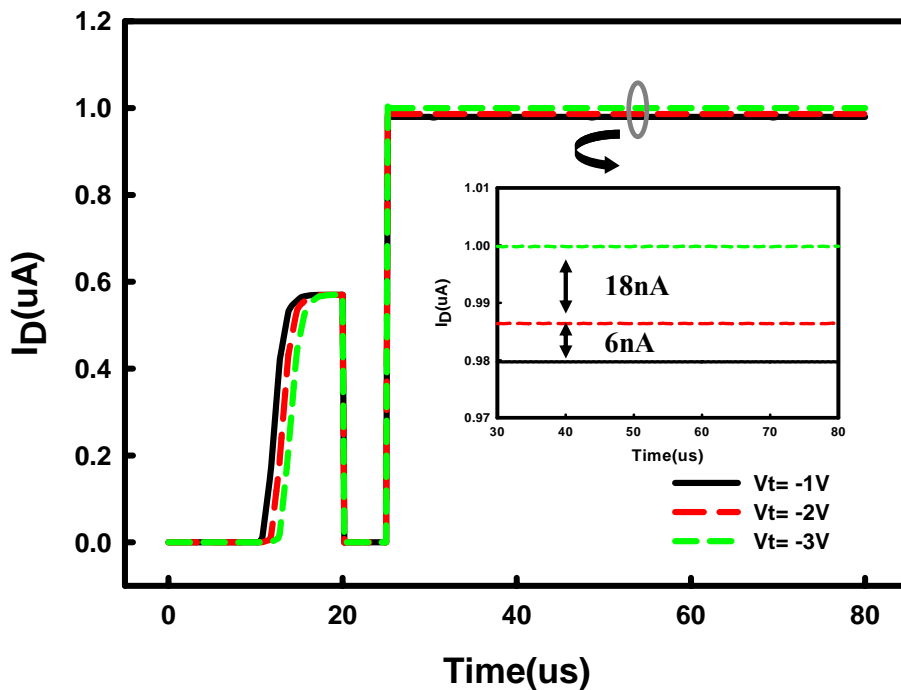


Fig.2-14 The change of driving current versus operation time with variant threshold voltage. Driving current was 0.98uA, 0.986uA, and 0.999uA corresponding to V_t = - 1. -2 and -3V

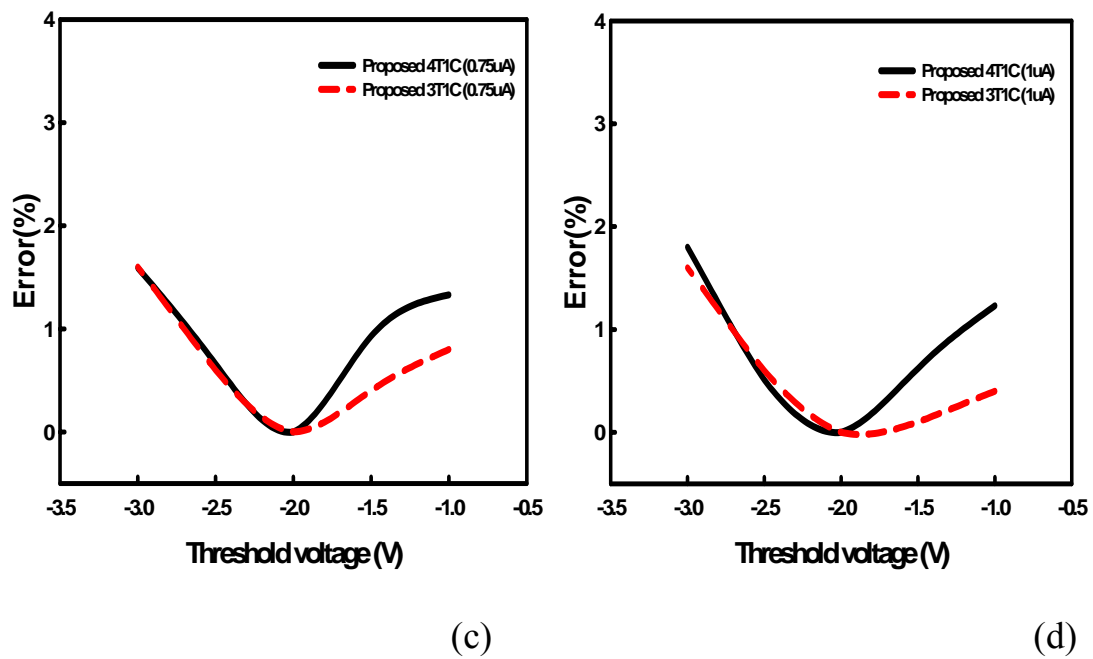
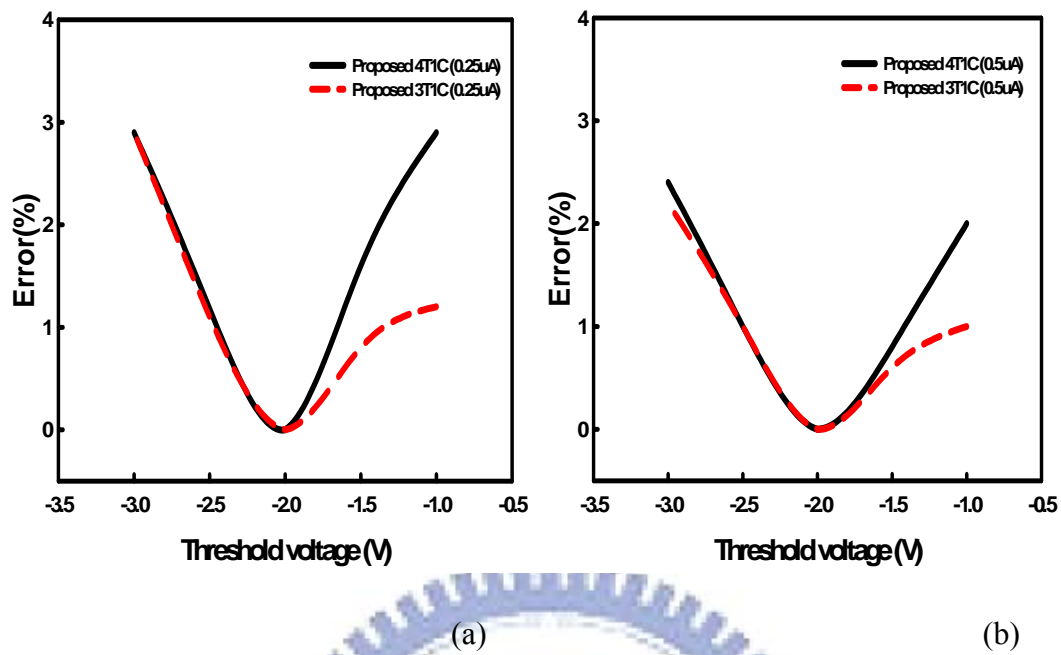
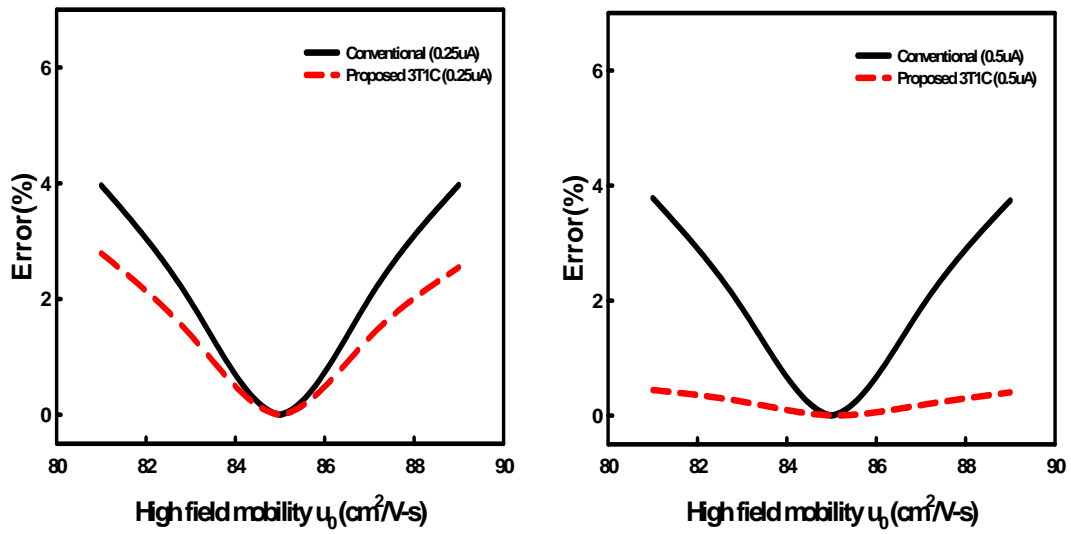
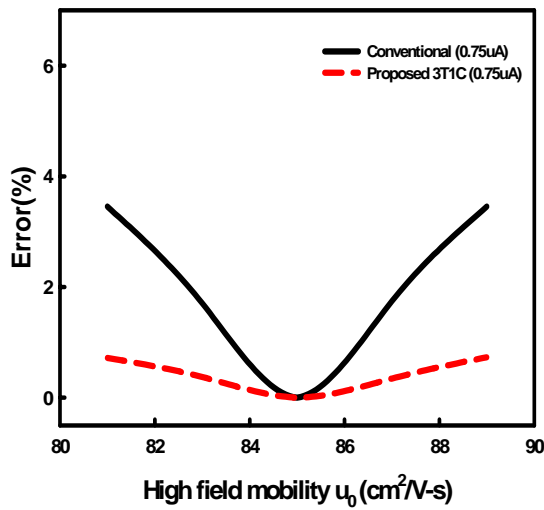


Fig 2-15 states current error versus threshold voltage among -2 ± 1 V with driving current (a) 0.25 μ A, (b) 0.5 μ A, (c) 0.75 μ A and (d) 1 μ A..

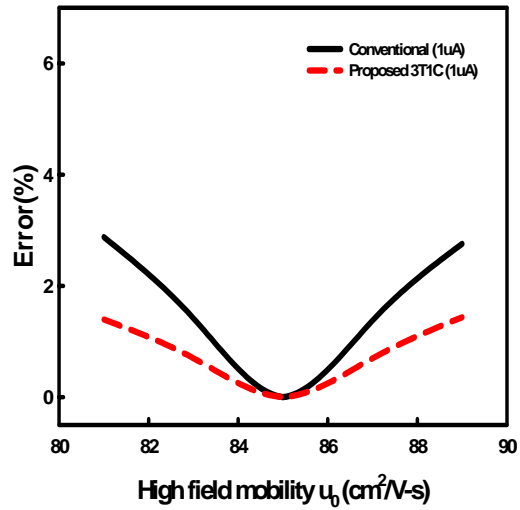


(a)

(b)



(c)



(d)

Fig 2-16 states current error versus mobility among $85 \pm 4 \text{ cm}^2/\text{V}\cdot\text{s}$ with driving current (a) 0.25uA, (b) 0.5uA, (c) 0.75uA and (d) 1uA..

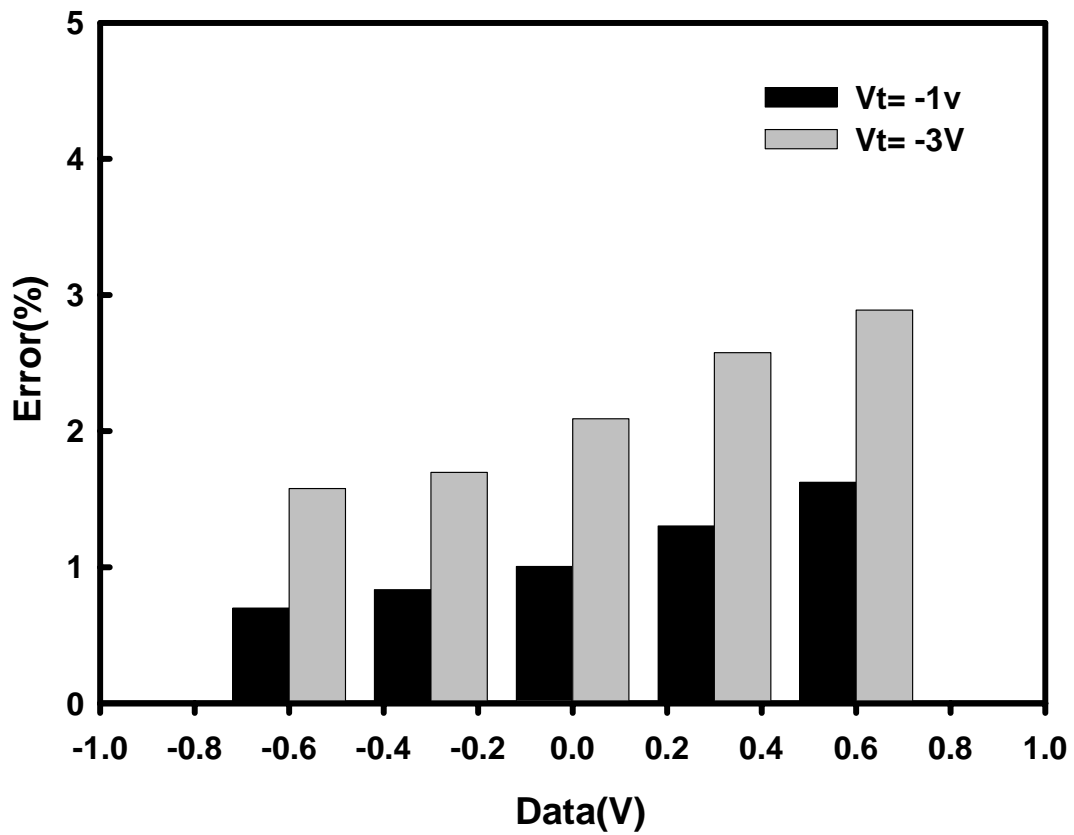


Fig.2-17 presents the current error of MD among the data range -0.6V~0.6V for threshold voltage -1V and -3V. Error rate is all less than 2.9% to reveal superior information of our study.

Chapter 3

Organic based compensation pixel circuit

3.1.1 Overview of OTFTs

Organic thin film transistors (OTFTs) have been widely studied because they have the potential for application in low cost, large area, flexible electronics [36][37]. OTFTs have been studied for low-cost applications, such as liquid crystal display panels, sensors, postage stamps, and radio-frequency identification[38]. Low-temperature processability allows a variety of low-cost substrate materials to be used, including flexible polymeric materials [38]. Most research related to the performance of OTFTs has focused on high mobility, low operating voltage, low subthreshold swing, and a threshold voltage close to 0 V [39]-[42]. In particular, the high operating voltage in the range of 20–100 V is a serious obstacle for realizing practical devices. A high operating voltage not only results in high power consumption and a high cost of the driving circuit but also damages the organic materials [41]. The key technique used to solve this problem concerns the gate insulator of OTFT. In order to induce larger number of carriers at a lower voltage, the gate insulator should be thinner and its dielectric constant should be larger [41].

3.1.2 Process Flow Of Organic Thin Film Transistors

Fabrication

a metal-oxide Al_2O_3 film layer was deposited on p-type (100) silicon wafers by E-gun evaporating system at room temperature. The thickness of as-deposited Al_2O_3 films was 240nm, which was measured by an

ellipsometer system. Subsequently, the wafers with 240nm-thick Al₂O₃ film were split into three groups, and processed with different post-treatments to study the properties of low-temperature-deposited Al₂O₃ film. Then, the samples were put into the oven with HMDS steam for 20mins at 150 °C. Pentacene was used as an active layer. This was deposited using ULVAC thermal evaporator. The deposition is started at a pressure lower than 3×10⁻⁶ torr. The deposition rate is controlled at 0.1Å/s. The temperature we use in depositing pentacene films is 70°C. We use shadow mask to define the active region of each device. The resulting thickness of the pentacene thin film was 70 nm, which was measured by a quartz-crystal thin film thickness monitor. After pentacene deposition, we deposited the gold (Au) which was thermally evaporated onto the pentacene film through a shallow mask to form the source and drain electrodes with normal channel width/length (W/L) = 800/200 μm. Finally, 300nm-thick Al gate electrodes were thermally evaporated on the backside of silicon wafers for the enhancement of gate voltage coupling.

3.1.3 Organic Thin Film Transistors Parameters Extraction

In this section, the methods of extraction the mobility, the threshold voltage, the on/off current ratio and the sub-threshold swing is characterized, respectively.

Mobility

Generally, mobility can be extracted from the transconductance in g_m the linear region:

$$g_m = \left[\frac{\partial I_D}{\partial V_G} \right]_{V_D=CONSTANT} = \frac{WC_{OX}}{L} \mu V_D \quad (3-1)$$

Mobility can also be extracted from the slope of the curve of the square-root of drain current versus gate voltage in the saturation region,

i.e. For $-V_D > -(V_G - V_T)$

$$\sqrt{I_D} = \sqrt{\frac{W}{2L} \mu C_{OX} (V_G - V_{TH})} \quad (3-2)$$

Threshold voltage

Threshold voltage is related to the operation voltage and the power consumptions of an OTFT. We extract the threshold voltage from equation (3-2), the intersection point of the square-root of drain current versus gate voltage when the device is in the saturation mode operation.

On/Off current ratio

Devices with high on/off current ratio represent large turn-on current and small off current. It determines the gray-level switching of the displays. High on/off current ratio means there are enough turn-on current to drive the pixel and sufficiently low off current to keep in low power consumption.

3.1.4 Measurement and SPICE model of OTFT

Fig.3-1 shows the cross-sectional view of a top contact & bottom gate OTFT structure, the fabrication and extraction of pentacene-based organic TFT devices is as followed before. Fig.3-2 (a) and (b) are the I_D - V_G and I_D - V_D of the experiment results respectively. The mobility of pentacene-based TFT device was $0.1 \text{ cm}^2/\text{V.s}$, threshold voltage -1.5V and on/off ratio 10^5 . The TFT RPI model for HSPICE simulation (Level=62) shows I_D - V_G in Fig3-3. The parameter of spice model is demonstrated below:

```

.MODEL PTFT PMOS (      LEVEL = 62

+TOX    = 2.4E-7      VTO    =P_VTH      RD    = 5.5E3

+RS     = 5.5E3      TNOM   = 27      ASAT  = 1.044

+AT     = 4.18496E-7  BLK    = 0.5546E-8    BT = 2.1267E-6

+DASAT  = 0          DD     = 4.7863E-7    DELTA = 4

+DG     = 6.91831E-8  DMU1   = 0          DVT   = 0

+DVTO   = 0          EB     = 0.68      ETA   = 10.31931

+I0     = 16.506     I00    = 191.3      LASAT = 0

+LKINK  = 2E-8      MC     = 3          MK    = 1.66

+MMU    = 2.44472   MU0    = 0.1      MU1   = 0.01

+MUS    = 2.51685   RDX    = 0          RSX   = 0

+VFB    = 0.1      VKINK  = 8          VON   = 0

+ACM    = 2        LD     = 5E-6     LDIF  = 0

+HDIF   = 3E-8     XL     = 0          RSH   = 7.61E3

+RSC    = 0        RDC    = 0          )

.PARAM  TEST2=AGAUSS(-1.5, 1 ,3 )

.PARAM  P_VTH=TEST2

```

Fig. 3-4 shows the measured and simulated characteristics of the OTFT devices. Comparisons show that the maximum RMS error of extracted physical quantities is less than 3% accuracy. However, compared with the I_D ($V_G = -20V$) has mismatch in deep saturation region due to the intrinsic limitation of the RPI TFT model. One of reason is that the RPI mobility function fails at the high gate bias conditions [42]. Therefore the mobility function loses the accuracy at the high gate biased condition. The error is increased when the gate bias is increased.

3.2 Complementary Voltage Induce Coupling Driving

3.2.1 Introduction

Pentacene-based organic TFTs (OTFTs) also have attracted lots of interest to be used for active-matrix organic light emitting diode (AMOLED) displays [18]-[20]. However, it has been reported that the OTFT device is subjected to environmental and bias stress instability [43], [44]. The threshold voltage variations of the OTFT device originated from manufacture processes and electrically biased operation are critical issues for the image quality of AMOLED panels over operation time. Besides, the OTFT exhibits a low mobility [45], [46] generally less than $0.5 \text{ cm}^2/\text{v.s}$, thus leading to the limit in the design of pixel circuitry. The development of compensation circuits suitable for the low-mobility OTFT architecture is, thereby, important to gain an proper electrical operation scheme and maintain a constant driving current for the OLED application. Nevertheless, few appropriate pixel circuits are presented for the OTFT-driving OLEDs in recent years, and most proposed circuits took advantage of the current driving schemes. The settling time issues [34] lead the current-driving scheme to set current data ranging from $2\mu\text{A}$ to $8\mu\text{A}$ [47], which are not realizable values for the AMOLED to define the gray scales. In this study, we propose a voltage-driving compensation circuit to well solve both issues of low mobility and threshold voltage variations for the OTFT-driving OLEDs.

3.2.2 Pixel structure and operation

Fig.3-5 depicts a schematic diagram of the proposed pixel circuitry. The inner of the dash square indicates a pixel region with a p-channel

driving OTFT device TD, and four switch OTFT transistors T1, T2, T3, and T4. The switch OTFT transistor T5 is designed to be outside the pixel area. The operation principle can be divided into three periods, including releasing charge, threshold voltage (V_t) generation and emission. In the first period, SCAN1 and SCAN2 are set to low to turn on the p-channel OTFTs T1, T2, and T3. T4 is in the powered off state and T5 is controlled at on state, respectively. In this period, the data voltage ($=V_{data}-V_{ref}$) is applied to node B (V_B), and node A (V_A) goes to $V_{EE}+V_{OLED}$. The layout of switch T5 was outside each pixel area and connected separately to each patterned cathode [48]. Therefore, the actual device layout in a pixel region consists of five transistors, especially suitable for the top-emission OLED pixel architecture. Such an arrangement of external driving circuit can decrease the manufacture complexity for each display pixel.

In the V_t generation period, SCAN1 is still kept low, T1 and T3 are kept in the turn-on state. SCAN2 goes high to turn T2 off, and T4 and T5 are changed to the on and off state, respectively. The data line is given $V_{DD}-V_{data}$. Because T4 is turned on and the voltage of data line changes, the voltage of node A (V_A) is suffered feed through [35] in the meanwhile and is boosted to a higher voltage level.

$$V_A = V_{EE} + V_{OLED} + (V_{DD} - (V_{data} - V_{ref})) \times \frac{C_{st}}{C_{st} + C_{OTFT}} + ((V_{DD} - V_{data}) - (V_{data} - V_{ref})) \times \frac{C_{OTFT}}{C_{st} + C_{OTFT}} \quad (3-3)$$

where $C_{st} \gg C_{OTFT}$, and C_{OTFT} is the parasitic capacitance of TD. For different input data, the corresponding threshold voltage generation period can be effectively decreased due to the voltage boost effect. It means a high level of data voltage in the first period, for example $V_{DD}=0V$, $V_{data}=15V$, and $V_{ref}=17V$, then $V_{DD}-(V_{data}-V_{ref})=2V$. The voltage of node A (V_A) has small boost effect. On the other hand, if a low level of

data voltage is given, it will produce relatively high boost effect. In this case, $V_{DD}=0V$, $V_{data}=2V$, and $V_{ref}=17V$, then $V_{DD}-(V_{data}-V_{ref})=15V$. The driving scheme is referred to as “Complementary Voltage Induce Coupling Driving” (CVICD). We also designed a single RC series circuit to verify the concept of the proposed CVICD. In this condition, $R=10\ \Omega$, $C=10\ \mu F$ and $V_s=10 \times u(t)\ V$, where $u(t)$ is a unit function. It takes 230 μs and 160 μs from an initial capacitor voltage of 0V and 5V to 9V (90% of V_s), respectively. The time difference between the two initial conditions is 70 μs . Thus, the CVICD method can decrease the charging time effectively. In the end of the V_t generation duration, V_A will be settle to $V_{DD}-V_{data}-|V_t|$.

In the driving period, SCAN1 is set to high to turn off T1 and T3. At the same time, SCAN2 is set to low to turn T2 on. Both T4 and T5 are at the on-state. At this moment, the source voltage of TD is V_{DD} , and then the voltage of storage capacitor is shown as followed.

$$V_A = V_{DD} - (V_{DD} - V_{data} - |V_t|) = V_{data} + |V_t|$$

$$I_{OLED} = K (V_A - |V_t|)^2 = K (V_{data} + |V_t| - |V_t|)^2 = K (V_{data})^2 \quad (3-4)$$

The above formula clearly indicates that the proposed compensation circuit includes higher immunity to the threshold voltage variation and especially suitable for OTFT-derived top-emission OLED pixel circuits.

3.2.3 Results and Discussion

In this work, the fabrication of pentacene-based organic TFT devices was as followed. A layer of 240 nm-thick Al_2O_3 film was electron-gun deposited on p-type silicon wafers. Then, a 70 nm-thick pentacene layer was thermally evaporated and patterned through a shallow mask at a rate of 0.5 $\text{\AA}/\text{sec}$. It was followed that a 100nm-thick gold (Au) layer was thermally evaporated onto the pentacene film through a shallow mask to form the source and drain electrodes with normal channel width/length

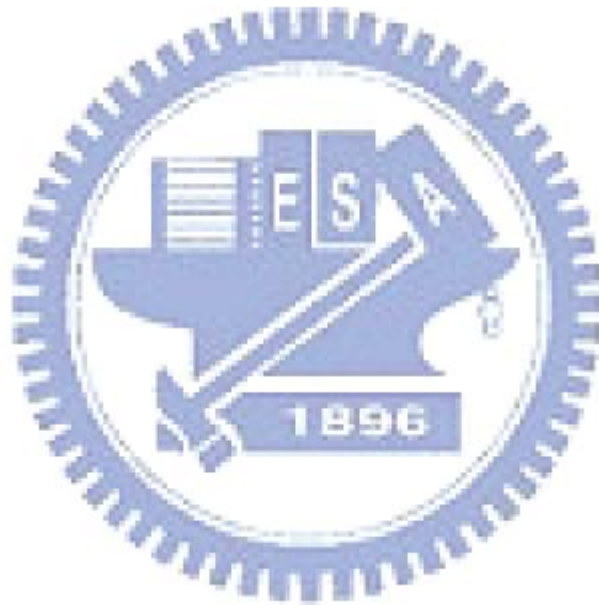
(W/L) = 800/200 μm . Finally, 300nm-thick Al gate electrodes were thermally evaporated on the backside of silicon wafers for the enhancement of gate voltage coupling. The mobility of pentacene-based TFT device was $0.1 \text{ cm}^2/\text{V}\cdot\text{s}$, threshold voltage -1.5V and on/off ratio 10^5 . The HSPICE software with the RPI model (Level=62) were used to verify the proposed OTFT pixel circuit. Fig.3-6 gives an information for V_t shift plot of our driving transistor model with $V_D = -10\text{V}$ and the shift value was between $\pm 1\text{V}$. Fig.3-7(a) shows the measured and simulated characteristics of the OTFT devices. Comparison among measured and simulated results is with good accuracy. We employed these modeling results for further circuit simulation. In this circuit simulation work, the ratio of channel width (W) to channel length (L) for TD was $300\mu\text{m}/50\mu\text{m}$, and switch T1 was $20\mu\text{m}/40\mu\text{m}$ designed to decrease the leakage current during the driving period, as well as other switch transistors were all set to $80\mu\text{m}/10\mu\text{m}$. The storage capacitor was 5 pF . Fig.3-7(b) shows the transition of driving current versus operation time for the OTFTs with variant threshold voltages in the proposed pixel circuit architecture. From Fig.3-7(c), the variation of driving current (ΔI) can be calculated is less than 1.8%. This result shows the proposed pixel circuit can produce the extremely similar driving current of OTFTs, independent of threshold voltage values. Fig.3-8(a) depicts the transient waveforms at specific nodes in the proposed pixel circuit while the input data was set to 5V for generating 262 nA of driving current. It is clearly observed an obvious voltage coupling effect, approximately 12V coupling voltage produced in a short time period. It indicates the charging period is shortened and effectively reduce the V_t generation time, which is especially suitable for the OTFT devices with the low mobility. Also, a less coupling effect is demonstrated while input data is set to 17V for generating 1 uA of driving current, as shown in Fig.3-8(b). The

evolution of coupling effect corresponding to the different input data voltages (e.g. 17V and 5V) is completely consistent with the proposed CVICD operation scheme. However, during the driving period (Regime III), Figs.3-8(a) and (b) show the value of TD source voltage (V_B) is -0.705V and -2.94V, separately, indicating V_B and V_C are deviated from the desirable V_{DD} level ($V_{DD}= 0$ V). It is inferred the OTFT devices do not exhibit good current swing in the linear operation region due to the presence of high turn-on resistance. These undesirable effects are mainly originated from the characteristics of OTFT devices. Therefore, it gives us a future work to improve the electrical performance of OTFT device. Fig.3-9 presents the current error of TD among the data range 1V~17V. It shows a good compensation function for the errors are all less than 2.9%. So, the circuit is really suitable for driving OTFT. Furthermore, Fig.3-10 represents output current of proposed pixel and conventional pixel at different threshold voltage shift. This simulation result showed that OLED current in proposed pixel degrades from 1uA to 0.973uA while OLED current in 2T1C conventional pixel degraded lower than 0.584uA, so the circuit really had excellent compensation ability to reduce the current nonuniformity.

3.2.4 Summary

we propose a novel active-matrix organic light-emitting diode displays (AMOLED) pixel circuit based on organic thin-film transistor (OTFT) architecture, which consisted of four switches, one driving transistor and a capacitor. The proposed voltage-driving pixel circuit, named as “Complementary Voltage Induced Coupling Driving” (CVICD), is different from the current-driving scheme and can appropriately operate at low gray level for the low-mobility OTFT circuitry. The current non-uniformity less than 2.9% for driving OLED is achieved by SPICE

simulation work successfully. The proposed operation scheme are especially suitable for the OTFT-based circuitry with low carrier mobility, by means of lowering the voltage drop between the source and drain terminals of OTFT device to narrow down the charging time. The current non-uniformity for driving OLED can be effectively reduced. Also, the adoption of the external driving can decrease one transistor in a pixel region and reduce the circuit complexity.



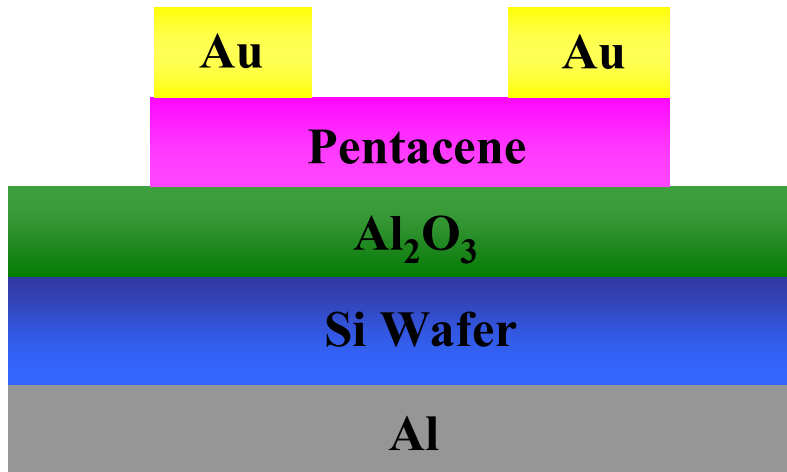


Fig. 3-1 shows the cross-sectional view of a top contact & bottom gate OTFT structure

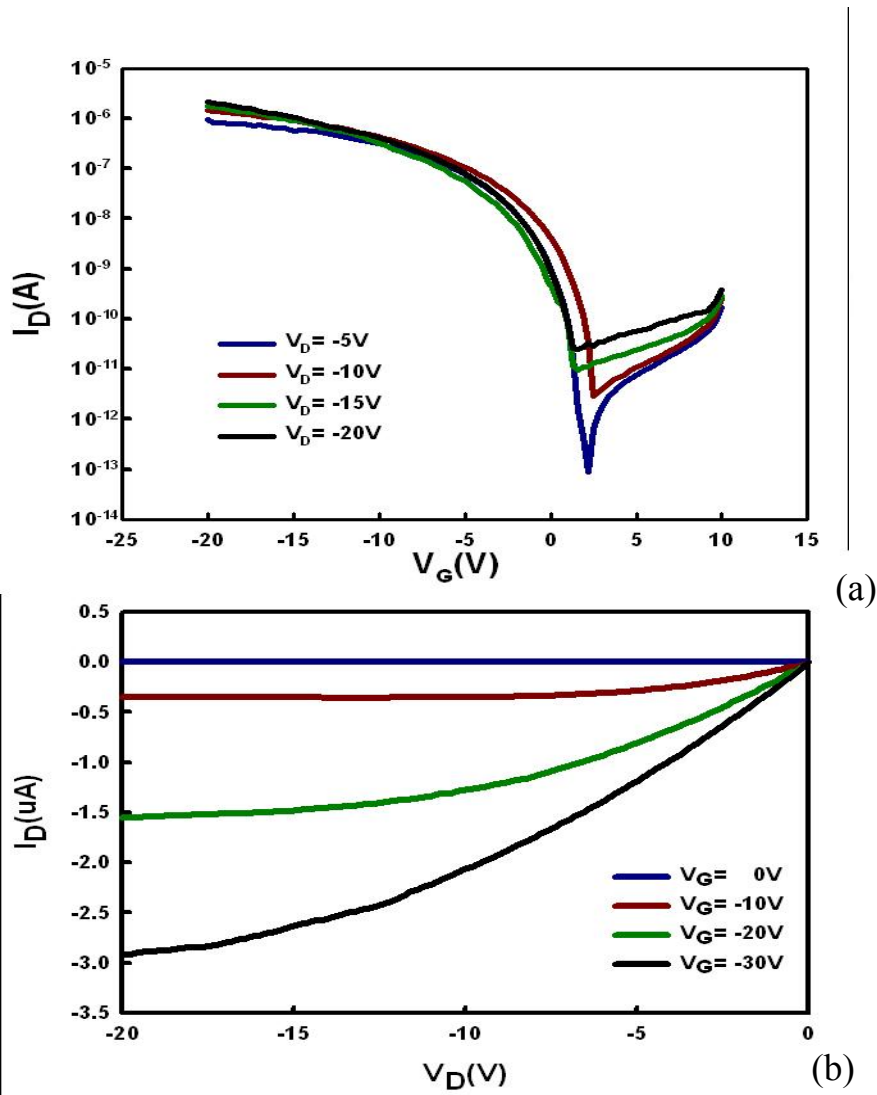


Fig. 3-2 (a) and (b) are the I_D - V_G and I_D - V_D of the experiment results respectively.

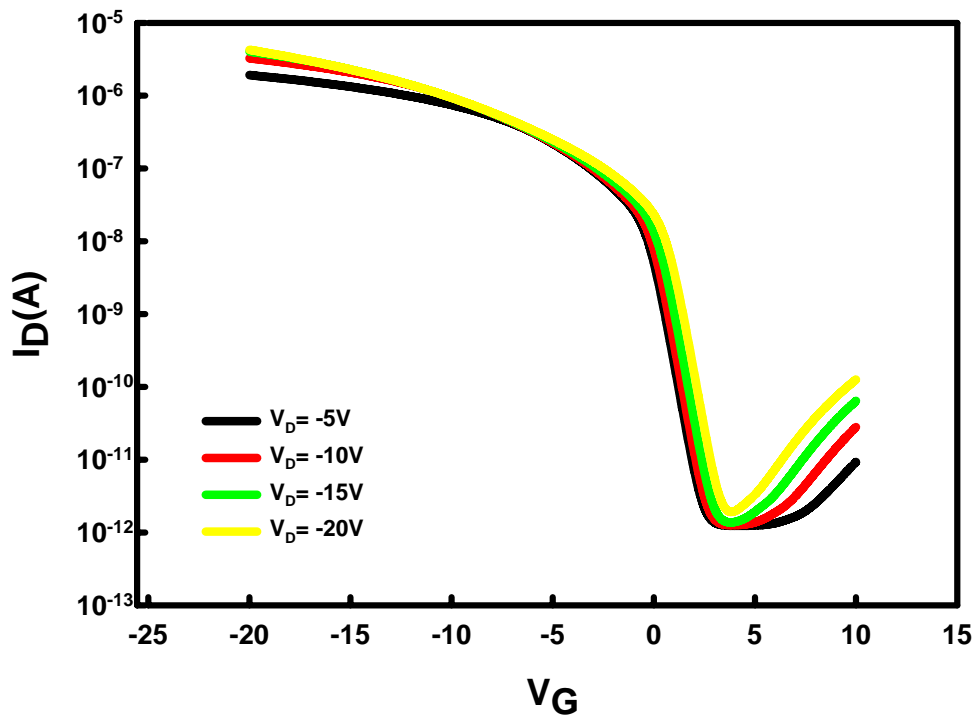


Fig. 3-3 The TFT RPI model for HSPICE simulation (Level=62) shows I_D - V_G plot.

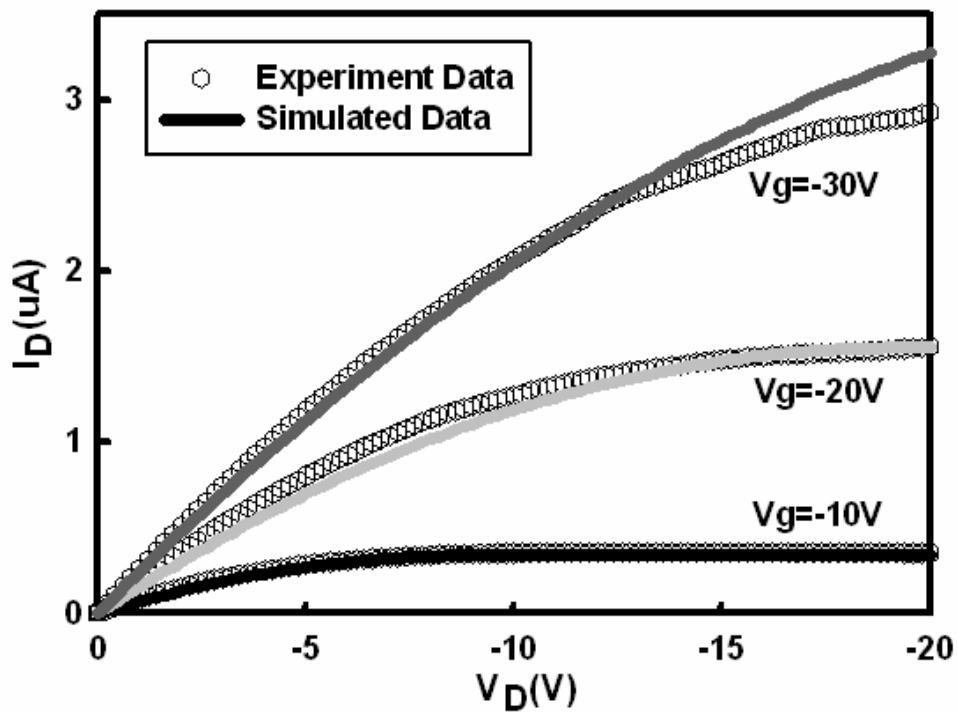


Fig. 3-4 shows the measured and simulated characteristics of the OTFT devices

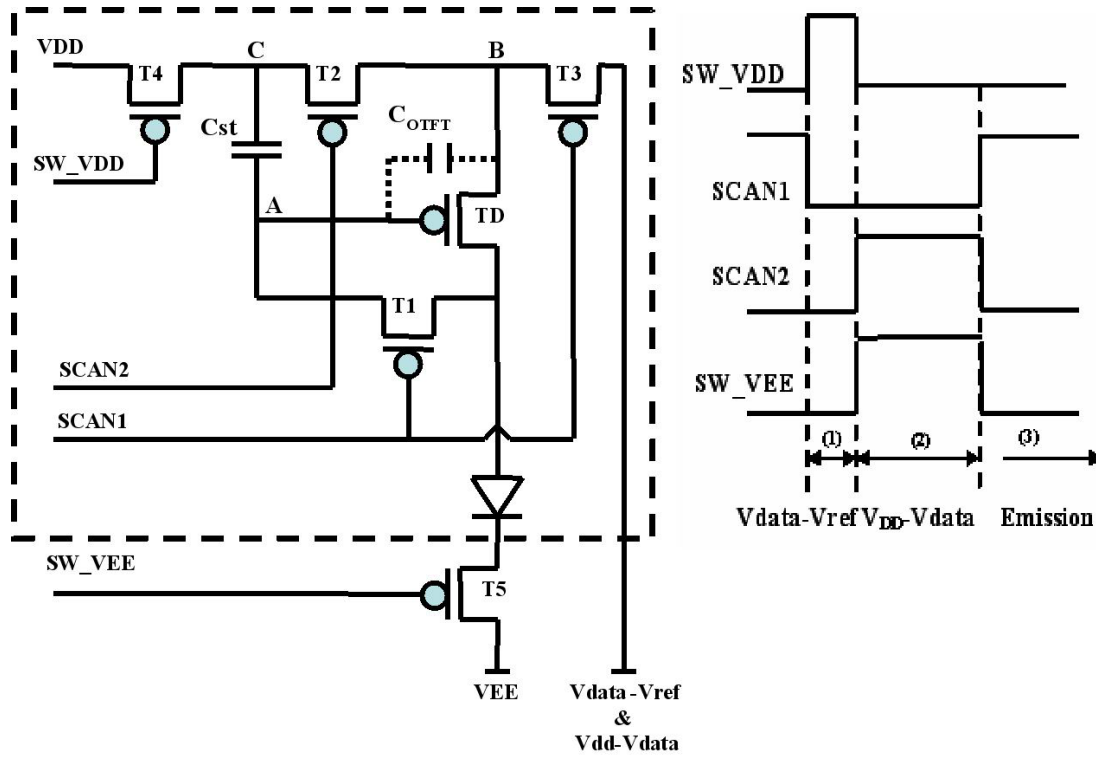


Fig.3-5 depicts a schematic diagram of the proposed pixel circuitry.

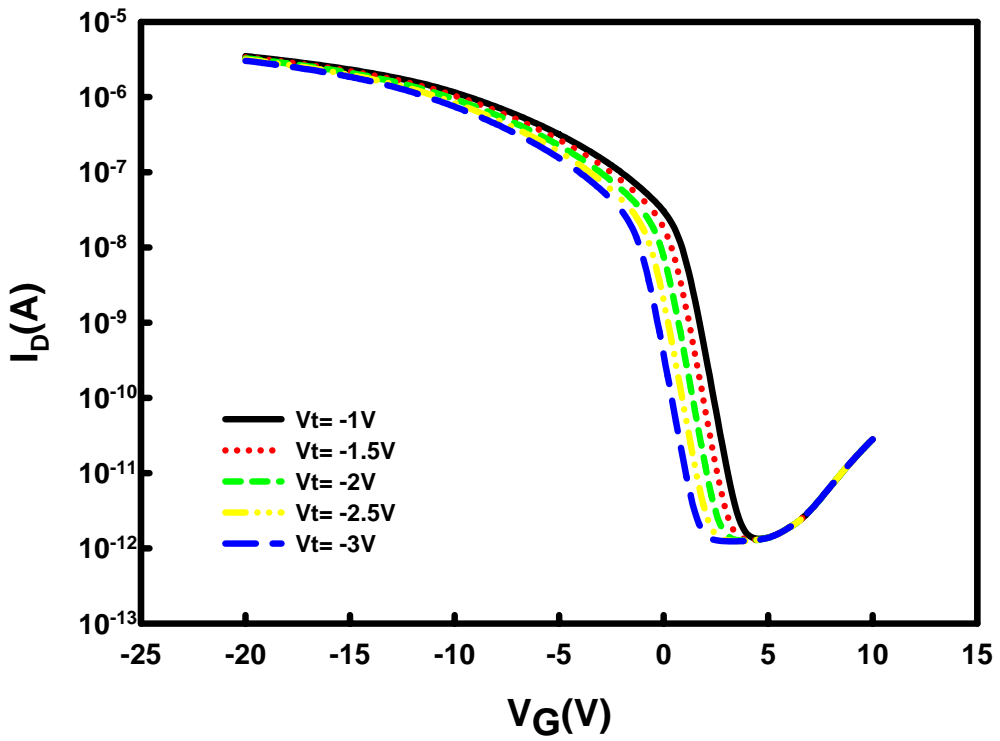


Fig.3-6 Vt shift plot of our driving transistor model with $V_D = -10V$ and the shift value is between $\pm 1V$

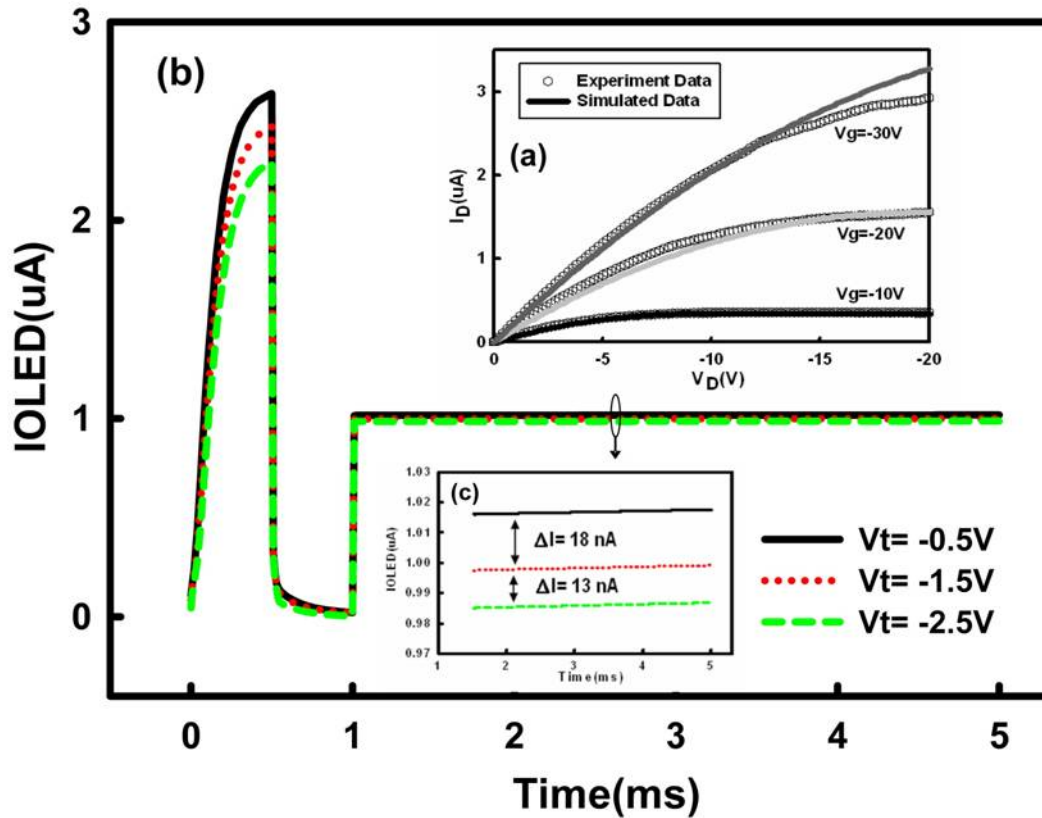


Fig.3-7(a) Measured and simulated output characteristics of pentacene-based OTFT for different gate voltage.(b) The change of driving current (IOLED) versus operation time for the OTFTs with variant threshold voltages in the proposed pixel circuit. IOLED is 1.016 uA, 0.998 uA and 0.9852 uA for $V_t = -0.5V$, $-1.5V$ and $-2.5V$, respectively. (c) The current ranging from 0.97 uA to 1.03 uA.

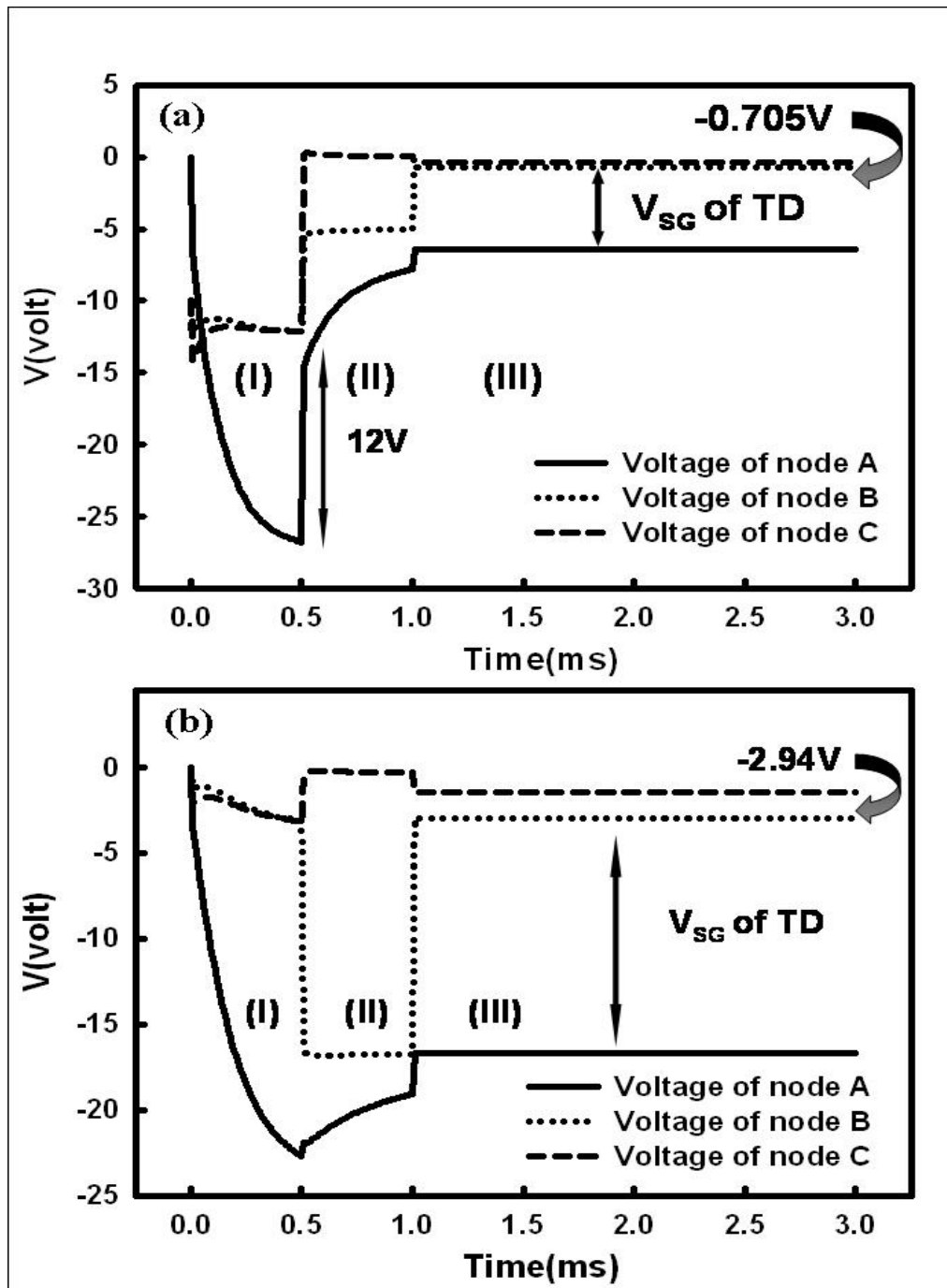


Fig. 3-8 Transient waveforms at specific nodes in the proposed pixel circuit while the input data was set to (a) $V_{data} = 5V$ for generating 262 nA of driving current, and (b) $V_{data} = 17V$ for generating 1 μA of driving current.

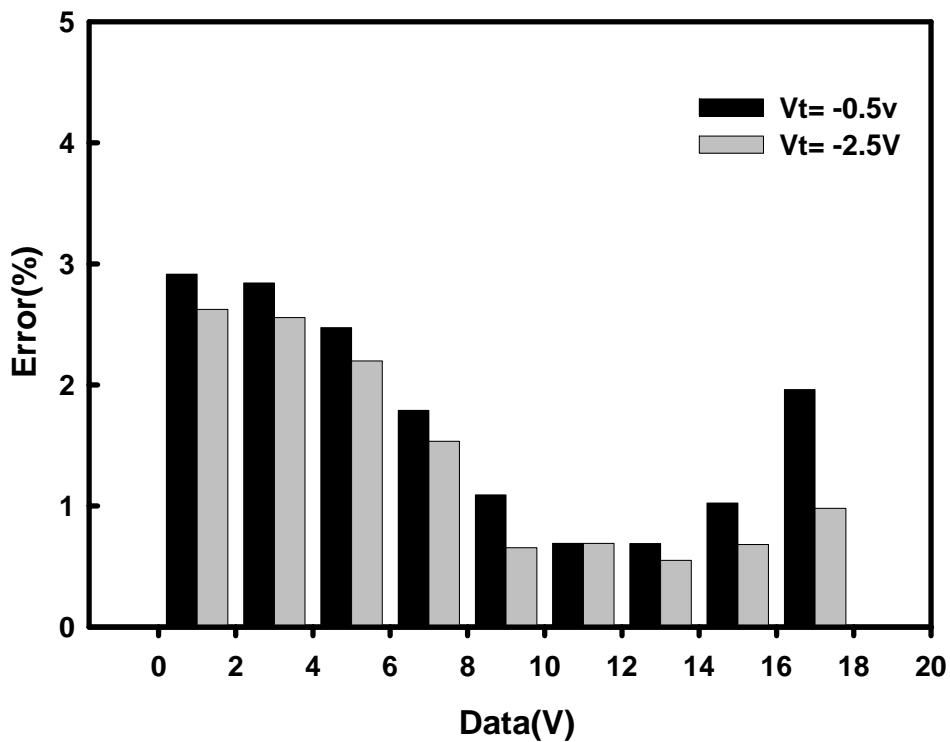


Fig.3-9 presents the current error of TD among the data range 1V~17V. It shows a good compensation function for the errors are all less than 2.9%.

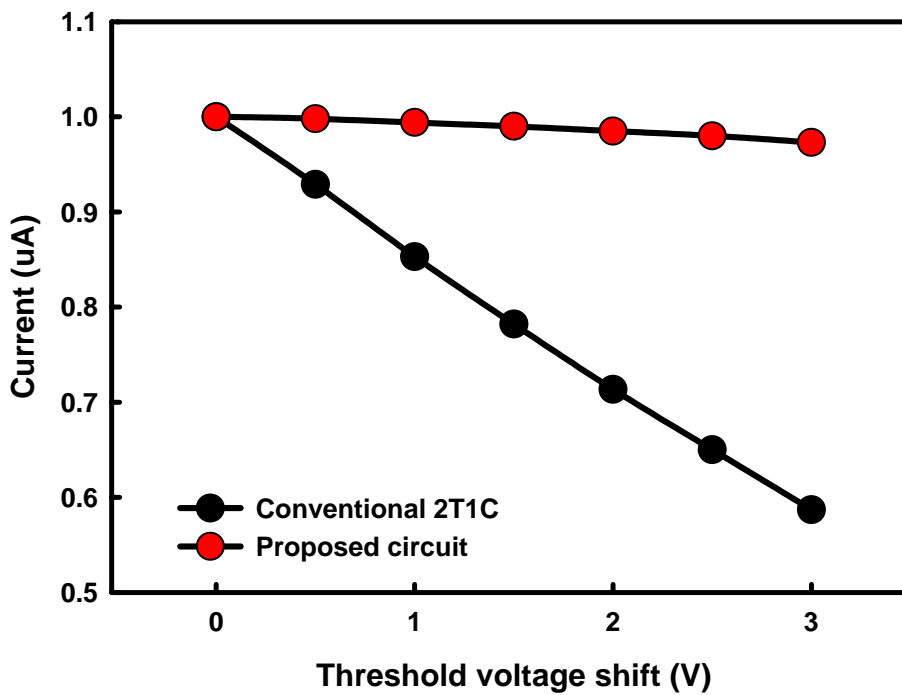


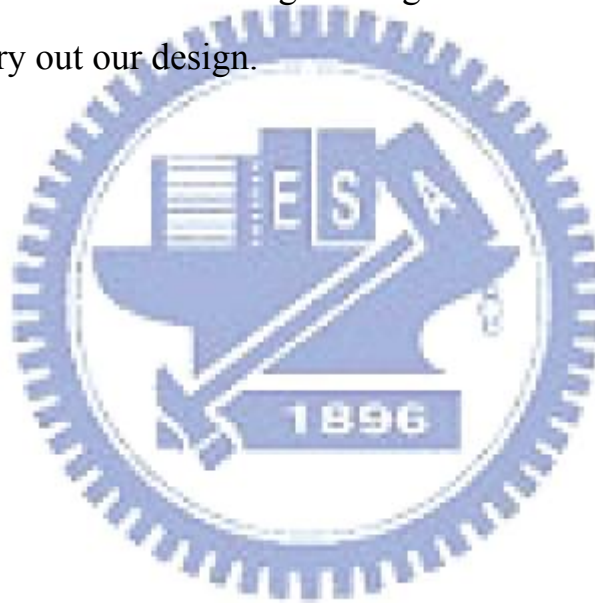
Fig.3-10 represents output current of proposed pixel and conventional pixel at different threshold voltage shift.

Chapter 4

Conclusions and Future works

AMOLED have attracted more attention in recent years. So far, . Conventional pixel circuit suffers substantially degradation. As a result, we have introduced three novel pixel circuits to overcome these drawbacks. Firstly, Simulation result of poly based pixel circuit is markedly better than conventional pixel circuit. Current error on 4T1C pixel circuit is 1.6% when the threshold voltage of the driving TFT shifts $\pm 1V$. Besides, a proposed new external driving method and we combine power & data line for driving can reduce the number of switch transistors in a pixel and circuit complexity. Secondly, a new hybrid driving scheme is proposed just with 3T1C and has comprehensive compensation function to reduce the effect of degraded TFT, and followed with a parallel driving method which could decrease the scanning time. Finally, we propose a novel circuit based on organic thin-film transistor (OTFT) architecture. The proposed voltage-driving pixel circuit, named as “Complementary Voltage Induced Coupling Driving” (CVICD), is different from the current-driving scheme and can appropriately operate at low gray level for the low-mobility OTFT circuitry. The current non-uniformity was less than 2.9%. The proposed operation scheme are especially suitable for the OTFT-based circuitry with low carrier mobility, by means of lowering the voltage drop between the source and drain terminals of OTFT device to narrow down the charging time. The current non-uniformity for driving OLED can be effectively reduced.

In the future, we will devote to practical implant the OTFT compensation circuit. Because the instable properties of OTFTs and large operation voltage for switch function give us plenty of obstacles to challenge. These undesirable effects are mainly originated from the characteristics of OTFT devices. Therefore, it gives us a future work to improve the electrical performance of OTFT device. Besides, the destination of AMOLED display based on all organic material is using plastic substrate for flexible using. Nevertheless, it produces another future work to us that is finding an organic insulator which can be patterned to carry out our design.



References

1. S. M. Sze, "Physics of Semiconductor Devices", Wiley, New York (1981).
2. M. Quirk and J. Serda, "Semiconductor Manufacturing Technology," Prentice-Hall, Inc., Upper Saddle River, New Jersey 07458. (2001)
3. Donald A. Neamen, "Fundamentals of Semiconductor Physics and Devices," McGraw-Hill, New York (1992)
4. 戴亞翔, "TFT-LCD 面板的驅動與設計 (Design and Operation of TFT-LCD Panels)," 五南圖書出版股份有限公司, Taiwan (2006)
5. 陳金鑫, 黃孝文, "OLED 有機電激發光材料與元件 (Organic Electroluminescent Materials & Devices)," 五南圖書出版股份有限公司, Taiwan (2005)
6. M. Stewart, R. S. Howell, L. Pires, M. K. Hatalis, W. Howard, and O. Parche, "Polysilicon VGA active matrix OLED displays-Technology and performance," in IEDM Tech.Dig.,1998, pp.871-874.
7. S. Luan and G.W. Neudeck, "An experimental study of the source/drain parasitic resistance effects in amorphous silicon thin film transistors," in J. Appl. Phys. 72(2) ,15 July 1992
8. S. Paul, A. J. Flewitt, W. I. Milne, and J. Robertson "Instability measurements in amorphous hydrogenated silicon using capacitance-voltage techniques," in Appl. Phys. Lett., 11 May 2005
9. Yue Kuo, "Thin film transistors material and process-Volume 1: Amorphous silicon thin film transistors," Kluwer Academic Publishers, Boston/Dordrecht/New York/London (2004)

10. S. Martin, C.S. Chiang, J.Y. Nahm, T. Li, J. Kanicki and Y. UGAI, "Influence of the Amorphous Silicon Thickness on Top Gate Thin-Film Transistor Electrical Performances," *Jpn.J.Appl.Phys.* Vol. 40(2001) pp.530-537
11. M.J.Powell, C. Van Berkel, and J.R.Hughes, "Time and temperature dependence of instability mechanisms in amorphous silicon thin film transistors," *Appl.Phys.Lett.*, vol.54, no.14, pp.1323-1325, 1989
12. Yue Kuo, "Thin film transistors material and process-Volume 2: Polycrystalline silicon thin film transistors," Kluwer Academic Publishers, Boston/Dordrecht/New York/London (2004)
13. John Y. W. Seto, "The electrical properties of polycrystalline silicon films," *J. Appl. Phys.*, vol.46, No. 12, Dec. 1975
14. G. Baccarani, B. Ricco and G. Spadini, "Transport properties of Polycrystalline silicon films," *J. Appl. Phys.* 49(11), Nov. 1978
15. J. Levinson, F.R. Shepherd, P. J. Scanlon, W. D. Westwood, G. Este, M. Rider, "Conductivity behavior in polycrystalline semiconductor thin film transistors" *J. Appl. Phys.* 53(2), Feb. 1982
16. K. R. Olasupo and M. K. Hatalis, "Leakage Current Mechanism in Sub-Micron Polysilicon Thin Film Transistors," *IEEE Trans. on Electron Devices*, vol. 43, No. 8, August 1996
17. Y. Uraoka, N. Hirai, H. Yano, T. Hatayama and T. Fuyuki, "Hot Carrier Analysis in Low-Temperature Poly-Si Thin Film Transistors Using Pico-Second Time-Resolved Emission Microscope," *Electron Device Letters*, vol. 24, No. 4, April 2003
18. T. Chuman, S. Ohta, S. Miyaguchi, H. Satoh, T. Tanabe, Y. Okuda, and M. Tsuchida, "Active matrix organic light emitting diode panel using organic thin-film transistors," presented at the Proc. Soc. Inf. Display, Settle, WA, May 23-28, 2004.
19. Y. Y. Lin, D. J. Gundlach, S. F. Nelson, and T. N. Jackson, "Stacked pentacene layer organic thin-film transistors with improved characteristics," *IEEE Electron Device Lett.*, vol. 18, no. 7, pp.

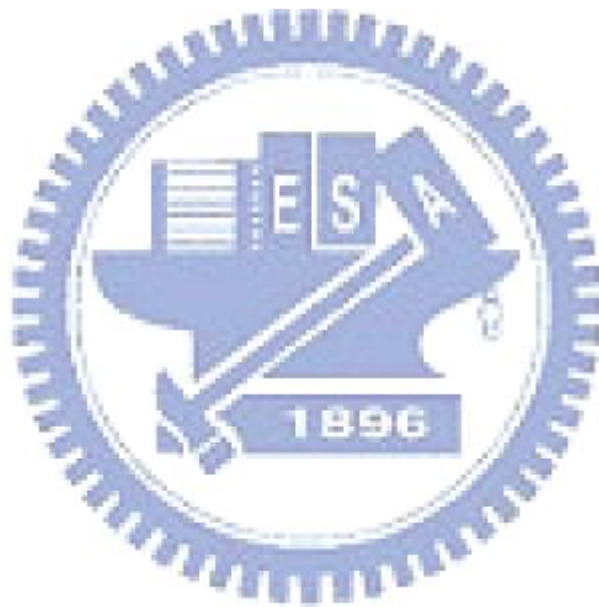
606-608, Jul, 1997.

20. L. Zhou, A. Wang, S. C. Wu, J. Sun, S. Park, and T. N. Jackson, "All-organic active matrix flexible display," *Appl. Phys. Lett.*, vol. 88, p. 083502, 2006.
21. M.A. Dawson and M.G. Kane, "Pursuit of active matrix organic light emitting diode displays," in *SID tech. Dig.*, 2001, pp. 372-375.
22. J.C. Goh, J. Jang, K.S. Cho, and C.K. Kim, "A new a-Si:H thin film transistor pixel circuit for active matrix organic light emitting diodes," *IEEE Electron Device Lett.*, vol. 24, no. 9, pp. 583-585, Sep. 2003.
23. S.H. Jung, W. J. Nam, and M.K. Han, "A new voltage-modulated AMOLED pixel design compensating for threshold voltage variation in poly-Si TFTs," *IEEE Electron Device Letts.*, vol. 25, no. 10, pp. 690-692, Oct. 2004.
24. J.H. LEE, W.J. Nam, S.H. Jung, and M.K. Han, "A new a-Si:H TFT pixel circuit compensating the threshold voltage shift of a-Si:H TFT and OLED for active matrix OLED," *IEEE Electron Device Lett.*, vol. 26, No. 12, pp. 897-899, Dec. 2005.
25. C.L. Lin and Y.C. Chen, "A novel LTPS-TFT pixel circuit compensating for TFT threshold voltage shift and OLED degradation for AMOLED," *IEEE Electron Device Lett.*, vol. 28, no. 2, pp. 129-131, Feb. 2007.
26. C.L. Lin and T.T. Tsai, "A novel Voltage Driving Method Using 3-TFT pixel Circuit for AMOLED," *IEEE Electron Device Lett.* Vol. 28, no. 6, June 2007.
27. Y. He, R. Horttori, and J. Kanicki, "Current-source a-Si:H TFT active-matrix organic light-emitting displays," *IEEE Electron Device Lett.*, vol. 21, pp. 590-592, Nov. 2000.
28. T. Sasaoka, M. Sekiya, A. Yumoto, J. Yamada, T. Hirano, Y. Iwase, T. Yamada, T. Ishibashi, T. Mori, M. Asano, S. Tamura, and T. Urabe, "A 13.0-inch AMOLED display with top emitting structure and adaptive current mode programmed pixel circuit (TAC)," in *Proc. SID*

- Tech. Dig.,2001, pp. 384-387.
- 29.H. Kageyama, H. Akimoto, Y. Shimizu, T. Ouchi, N. Kasai, H. Awakura, N. Tokuda, K. Kajiyama, and T. Sato, “A 2.5-inch OLED Display with a Three-TFT Pixel Circuit for Clamped Inverter Driving”, SID’04 Digest, p.1394-1397(2004)\
 30. H. Kageyama, H. Akimoto, T. Ouchi, N. Kasai, H. Awakura, N. Tokuda, and T. Sato, “A 3.5-inch OLED Display using a 4-TFT Pixel Circuit with an Innovative Pixel Driving Scheme”, SID’03 Digest, p.96-99(2003)
 31. A. Nathan, **G.R. Chaji**, and S.J. Ashtiani, "Driving schemes for a-Si and LTPS AMOLED displays," *IEEE J. of Display Technology*, vol. 1, no. 2, pp. 267-277, Dec. 2005.
 32. M. Stewart, R. S. Howell, L. Pires, M. K. Hatalis, W. Howard, and O. Parche, “Polysilicon VGA active matrix OLED displays—Technology and performance,” in *IEDM Tech. Dig.*, 1998, pp. 871–874
 33. A. Asano, T. Kinoshita, and N. Otani, “A plastic 3.8-in low-temperature polycrystalline silicon TFT color LCD panel,” in *Proc. SID Dig.*, May 2003, vol. 34, no. 1, pp. 988–99
 34. G. R. Chaji, and A. Nathan, ”Parallel addressing scheme for voltage-programmed active-Matrix OLED displays” *IEEE Trans. Electron Devices*, vol. 54, Issue 5, pp 1095-1100, May 2007.
 35. B. J. Sheu and C. Hu, “Switch-induced error voltage on a switched capacitor,” *IEEE J. Solid-State Circuits*, vol. SC-19, no. 4, pp. 519–525, Aug. 1984
 - 36.L. A. Majewski, R. Schroeder, and M. Grell, “One volt organic transistor”, *Adv. Mater. (Weinheim, Ger.)*, vol. 17, pp. 192, 2005.
 - 37.H. Klauk, D. J. Gundlach, J. A. Nichols, and T. N. Jackson, “Pentacene organic thin-film transistors for circuit and display applications”, *IEEE Trans. Electron Devices*, vol. 46, pp. 1258, 1999.

38. D. J. Gunlach, L. Jia, and T. N. Jackson, "Pentacene TFT with Improved Linear Region Characteristics using Chemically Modified Source and Drain Electrodes", *IEEE Electron Device Lett.*, vol. 22, pp. 571, 2001.
39. J. B. Koo, S. J. Yun, J. W. Lim, S. H. Kim, C. H. Ku, S. C. Lim, J. H. Lee, and T. Zyung, "Low-voltage and high-gain pentacene inverters with plasma-enhanced atomic-layer-deposited gate dielectrics", *Appl. Phys. Lett.*, vol. 89, 033511, 2006.
40. C. D. Dimitrakopoulos, S. Purushothaman, J. Kymissis, A. Callegari, and J. M. Shaw, "Low-Voltage Organic Transistors on Plastic Comprising High-Dielectric Constant Gate Insulators", *Science*, vol. 283, pp. 822, 1999.
41. Y. Iino, Y. Inoue, Y. Fujisaki, H. Fujikake, H. Sato, M. Kawakita, S. Tokito, and H. Kikuchi, "Organic Thin-Film Transistors on a Plastic Substrate with Anodically Oxidized High-Dielectric-Constant Insulators", *Jpn. J. Appl. Phys., Part 1*, vol. 42, pp. 299, 2003.
42. L. A. Majewski, R. Schroeder, and M. Grell, "Low-voltage, high-performance organic field-effect transistors with an ultra-thin TiO₂ layer as gate insulator", *Adv. Funct. Mater.*, vol. 15, pp. 1017, 2005.
43. Y. Hun, G. Dong, Y. Liang, L. Wang and Y. Qiu, "Research on operating degradation of pentacene thin-film transistor," *Jan. J. of Applied Physics*, vol. 44, no. 29, pp. L938-L940, 2005.
44. T. Sekitani, S. Iba, Y. Kato, Y. Noguchi, and T. Someya, "Suppression of DC bias stress-induced degradation of organic field-effect transistors using postannealing effects," *Appl. Phys. Lett.*, vol. 87, p. 073505, 2005.
45. C. W. Chu, C. W. Chen, S. H. Li, and Y. Yanga, "Integration of organic light-emitting diode and organic transistor via a tandem structure," *Appl. Phys. Lett.*, vol. 86, p. 253503, 2005.
46. M. G. Kane, I. G. Hill, J. Campi, M. S. Hammond, and B. Greening, "AMLCDs using organic thin-film transistors on polyester substrates," in *SID DIGEST*, 2001, pp. 57-59.

47. A. Shin, S. J. Hwang, S. W. Yu, and M. Y. Sung, "A new organic thin-film transistor based current-driving pixel circuit for active-matrix organic light-emitting displays," in 8th International Symposium on Quality Electronic Design (ISQED'07), 2007, pp. 59-66
48. C Liu, G Zhu, D Liu," Patterning cathode for organic light-emitting diode by pulsed laser ablation", Displays, 2008 - Elsevier



學經歷

姓名：竹立煒

性別：男

生日：民國七十三年七月二十日

地址：300 新竹市東大路二段 239 巷一弄 3 號 3 樓

學歷：國立新竹高中 (88.9~91.6)

國立中山大學電機工程學系學士 (91.9~95.6)

國立交通大學光電工程所碩士班 (95.9~97.6)

碩士班論文題目：主動矩陣有機發光二極體於薄膜電晶體之補償驅動
電路研究

(Research of AMOLED pixel compensation circuit using TFTs)